Biodiversity and Conservation manuscript No.
(will be inserted by the editor)

Remote sensing for biodiversity monitoring: A review of methods for biodiversity indicator extraction and assessment of progress towards international targets

Zisis I. Petrou · **Ioannis Manakos** · **Tania Stathaki**

Received: 26 January 2015 / Accepted: 15 June 2015

Abstract Recognizing the imperative need for biodiversity protection, the Convention on Biological Diversity (CBD) has recently established new targets towards 2020, the so-called Aichi targets, and updated proposed sets of indicators to quantitatively monitor the progress towards these targets. Remote sensing has been increasingly contributing to timely, accurate, and cost-effective assessment of biodiversity-related characteristics and functions during the last years. However, most relevant studies constitute individual research efforts, rarely related with the extraction of widely adopted CBD biodiversity indicators. Furthermore, systematic operational use of remote sensing data by managing authorities has still been limited. In this study, the Aichi targets and the related CBD indicators whose monitoring can be facilitated by remote sensing are identified. For each headline indicator a number of recent remote sensing approaches able for the extraction of related properties are reviewed. Methods cover a wide range of fields, including: habitat extent and condition monitoring; species distribution; pressures from unsustainable management, pollution and climate change; ecosystem service monitoring; and conservation status assessment of protected areas. The advantages and limitations of different remote sensing data and algorithms are discussed. Sorting of the methods based on their reported accuracies is attempted, when possible. The extensive literature survey aims at reviewing highly performing methods that can be used for large-area, effective, and timely biodiversity assessment, to encourage the more systematic use of remote sensing solutions in monitoring progress towards the Aichi targets, and to decrease the gaps between the remote sensing and management communities.

Keywords biodiversity indicator · remote sensing · indicator estimation · Aichi Targets · CBD biodiversity indicators · ecosystem monitoring

Z. I. Petrou · T. Stathaki
Department of Electrical and Electronic Engineering, Imperial College London, South Kensington Campus, London, SW7 2AZ, United Kingdom
E-mail: z.petrou10@imperial.ac.uk

Z. I. Petrou · I. Manakos
Information Technologies Institute, Centre for Research and Technology Hellas, P.O. Box 60361, 6th km Xarilaou - Thermi, 57001, Thessaloniki, Greece
Tel.: +30-2311-257711, Fax: +30-2310-474128

1 Introduction

Biodiversity is a key factor for ecosystem stability and functioning, severely affecting human society and health (Cardinale et al. 2012; Balvanera et al. 2006). It is a complex notion, difficult to measure explicitly (Gillespie et al. 2008; Duro et al. 2007). Various indicators are used to assess the status and trends of components of biodiversity, measure pressures, and quantify biodiversity loss at the level of genes, populations, species, and ecosystems, at various scales (Butchart et al. 2010; EEA 2007; Duelli and Obrist 2003). Several sets of such indicators have been proposed by organizations, scientists, and policy makers (Feld et al. 2009; Strand et al. 2007; EEA 2007; Kati et al. 2004; Lindenmayer et al. 2000; Jonsson and Jonsell 1999). They can be either directly measured or calculated using statistical models and may have a global, regional, or national applicability. Among the most widely adopted sets are the ones proposed by the United Nations (UN) Convention on Biological Diversity (CBD), aiming at monitoring the progress towards the achievement of the defined targets at global scale (2010BIP 2010; AHTEG 2011). Further efforts include the definition of more directly measured variables, to enhance indicator extraction, such as the Essential Biodiversity Variables (EBV) proposed by the Group on Earth Observations Biodiversity Observation Network (GEO BON) (Pereira et al. 2013).

The imperative need for biodiversity protection has been highlighted lately (Brooks et al. 2006), with the UN declaring 2010 as the International Year of Biodiversity and 2010–2020 as the Decade on Biodiversity. Realizing that the targets for halting biodiversity loss by 2010 were not met (CBD 2010; Butchart et al. 2010), CBD and the European Union (EU) updated their mitigation strategies towards 2020 (CBD 2012; EEA 2012b). CBD adopted the Strategic Plan for Biodiversity 2011–2020 and set the so-called Aichi Biodiversity Targets (CBD 2012), as criteria of achieving the defined goals by 2020.

Although in-situ campaigns are the most accurate way of measuring certain aspects of biodiversity, such as the distribution and population of plant and animal species, in many cases, they are proven particularly costly, time demanding, or impossible (Buchanan et al. 2009; Gong et al. 2007). Remote sensing (RS) data, on the contrary, from airborne or satellite sensors, are increasingly employed in biodiversity monitoring studies (Nagendra et al. 2013; Bergen et al. 2009; Gillespie et al. 2008; Turner et al. 2003). Offering repetitive and cost-efficient monitoring of large areas, RS data can provide precious information nearly impossible to be acquired by field assessment alone (Nagendra 2001). Numerous studies using RS data to measure biodiversity-related properties are presented in the literature, covering a broad range of applications, study areas, data and methods.

However, most studies are rarely explicitly connected to any widely adopted biodiversity indicator that could be extracted through them directly or indirectly. Instead, various indicators have been used by individual studies, resulting in numerous incompatible monitoring systems (Feld et al. 2009). Furthermore, despite the increasing availability of RS data, the connection between variables measured by RS and indicators required by the biodiversity and policy-making community is still poor (Secades et al. 2014). Thus, a link of RS approaches to a common set of indicators would be highly beneficial and is attempted in this study.

A contribution of the study is the identification of Aichi targets whose progress can be monitored through RS data, by distinguishing the biodiversity indicators and EBVs that can be extracted using such data. Furthermore, a large number of state-of-the-art RS studies monitoring different biodiversity-related variables with satellite and airborne sensors are reviewed. A range of applications covering all RS related CBD headline indicators are included. A link of the methods to the CBD indicators whose extraction can be facilitated with

their use is provided. Evaluation of the methods based on their outcomes and the achieved accuracies, when appropriate, is undertaken identifying the best performing ones. Based on the discussion on used sensors and processing algorithms, the study attempts to provide a useful tool for researchers and policy makers to select the most appropriate method for the extraction of CBD biodiversity indicators, in either local or global scale.

2 Earth Observation for biodiversity monitoring

CBD initially suggested a set of biodiversity indicators to monitor the progress of biodiversity conservation by 2010, the so-called 2010 Biodiversity Target (Strand et al. 2007). The indicators were globally applicable and organized in seven focal areas, ranging from conservation and sustainable use of biodiversity to social considerations dependent upon its maintenance. Failing to meet the 2010 targets (Butchart et al. 2010), new indicators and an updated organization of all biodiversity indicators under 12 headline indicators were proposed (AHTEG 2011), meant to monitor the progress towards the achievement of the 20 Aichi Targets (CBD 2012).

Upon demand by CBD, GEO BON attempted to assess the adequacy of global observation systems, mainly on information capacity, for monitoring biodiversity and the achievement of the Aichi targets (GEO BON 2011). Although numerous existing systems were identified, developing and funding them is needed to achieve global targets. Acknowledging the lack (Pereira et al. 2012) and envisaging the development of a global harmonized system to observe biodiversity (Scholes et al. 2012), a set of candidate EBVs were suggested (Pereira et al. 2013). They aim at defining a minimum set of essential measurements and acting as an intermediate layer between primary observations (e.g. RS data) and biodiversity indicators, facilitating the extraction of the latter. Six main EBV classes have been defined, with the particular EBVs being under development (Pereira et al. 2013).

In addition, several biodiversity-related international projects have recently been implemented, such as the 7th European Framework Programme (FP7) EU_BON (Building the European Biodiversity Observation Network – http://www.eubon.eu), MS.Monina (Multi-scale Service for Monitoring Natura 2000 Habitats of European Community Interest – http://www.ms-monina.eu), and BIO_SOS (BIOdiversity multi-SOurce monitoring System: From Space to Species – http://www.biosos.eu); the latter two focusing on biodiversity monitoring from space. RS is expected to contribute immensely in assessing the progress towards certain Aichi targets, by extracting and updating the respective CBD indicators or related EBVs. Table 1 identifies the CBD headline indicators that may be extracted through RS data, and the mainly associated Aichi targets. Relevant EBV classes are also reported.

Table 1 Aichi targets that can be monitored through RS data, and the associated CBD headline indicators (AHTEG 2011) and EBV classes (Pereira et al. 2013). The index numbers of the Aichi targets and CBD indicators used in their definition documents are given in parenthesis. Abbreviations of CBD headline indicators: (1) Extent: Trends in extent, condition, and vulnerability of ecosystems, biomes, and habitats; (2) Species: Trends in abundance, distribution, and extinction risk of species; (4) Pressures practices: Trends in pressures from unsustainable agriculture, forestry, fisheries, and aquaculture; (5) Pressures various: Trends in pressures from habitat conversion, pollution, invasive species, climate change, overexploitation, and underlying drivers; (6) Services: Trends in distribution, condition, and sustainability of ecosystem services for equitable human well-being; (11) Protected areas: Trends in coverage, condition, representativeness, and effectiveness of protected areas and other area-based approaches.

Aichi targets	CBD headline indicators	EBV classes
(4) Sustainable production and consumption	(4) Pressures practices (5) Pressures various	Species populations
(5) Reduction of habitat loss, fragmentation and degradation	(1) Extent (4) Pressures practices (5) Pressures various	Species populations Ecosystem function Ecosystem structure
(6) Sustainable exploitation of marine resources	(4) Pressures practices	Species populations
(7) Sustainable management of agriculture, aquaculture and forestry areas	(4) Pressures practices	Species populations Ecosystem structure
(8) Pollution reduction	(5) Pressures various	Species populations Community composition Ecosystem function
(9) Invasive alien species control	(2) Species (5) Pressures various	Species populations
(10) Protection of vulnerable ecosystems	(5) Pressures various	Species populations Community composition Ecosystem structure
(11) Conservation and protection of important areas	(11) Protected areas	Species populations Ecosystem structure
(12) Preventing extinction of threatened species	(2) Species	Species populations
(14) Safeguarding ecosystems with essential services	(6) Services (11) Protected areas	Species populations Community composition Ecosystem function Ecosystem structure
(15) Enhancing ecosystem resilience	(6) Services (11) Protected areas	Species populations Species traits Ecosystem structure

3 Remote sensing capacity for CBD indicator extraction

Extending previous studies focusing on policy makers and identifying the principal role of RS data in CBD indicator extraction (Secades et al. 2014), the present study focuses not only on the potential of various RS data, but also on the data processing and mapping algorithms. A variety of measures, defined in Table 2, have been employed to evaluate the accuracy of the methods cited in this study, depending on the characteristics of each method and the nature of the problem. An indicative sorting of the methods is attempted for each category of measured variables, although an indisputable comparison of the methods would

Table 2 Accuracy evaluation measures used in the methods cited in this study.

Metric	Definition	Symbols
Overall accuracy	$OA \equiv \frac{NC}{N}$	NC: number of correctly classified samples; N: total number of samples
Producer's accuracy (for class A)	$PA_A \equiv \frac{NC_A}{NO_A}$	NC_A: Correctly classified samples to class A; NO_A: total observed samples of class A
Omission error (for class A)	$EO_A \equiv 1 - PA_A$	
User's accuracy (for class A)	$UA_A \equiv \frac{NC_A}{NP_A}$	NC_A: Correctly classified samples to class A; NP_A: total samples classified to class A
Commission error (for class A)	$EC_A \equiv 1 - UA_A$	
Cohen's kappa coefficient	$\kappa \equiv \frac{P_o - P_c}{1 - P_c}$	P_o: proportion of agreement between classified and observed samples $\equiv OA$; P_c: proportion of expected agreement by chance, $P_c = \sum_{i=1}^{C}(NO_i/N)(NP_i/N)$, C: number of classes, NO_i, NP_i, N defined as above
Pearson's correlation coefficient	$r \equiv \frac{\sum_{i=1}^{N}(f_i - \bar{f})(y_i - \bar{y})}{\sqrt{\sum_{i=1}^{N}(f_i - \bar{f})^2}\sqrt{\sum_{i=1}^{N}(y_i - \bar{y})^2}}$	y_i: observed values; f_i: model predicted values; $\bar{y} \equiv \sum_{i=1}^{N} y_i/N$; $\bar{f} \equiv \sum_{i=1}^{N} f_i/N$; N: number of samples
Coefficient of determination	$R^2 \equiv 1 - \frac{\sum_{i=1}^{N}(y_i - f_i)^2}{\sum_{i=1}^{N}(y_i - \bar{y})^2}$	y_i, f_i, $\bar{y}$, N defined as above
Adjusted R^2	$\bar{R}^2 \equiv R^2 - (1 - R^2)\frac{D}{N - D - 1}$	N: number of samples; D: number of explanatory variables in the regression model
Root mean square error	$\mathrm{RMSE} = \sqrt{\frac{1}{N}\sum_{i=1}^{N}(y_i - f_i)^2}$	y_i, f_i, N defined as above
Absolute (standard) error	$E = \frac{1}{N}\sum_{i=1}^{N}\lvert y_i - f_i\rvert$	y_i, f_i, N defined as above
Relative (standard) error	$E_r = \frac{1}{N}\sum_{i=1}^{N}\frac{\lvert y_i - f_i\rvert}{y_i}$	y_i, f_i, N defined as above

only be possible if experiments were conducted under the same conditions, datasets, or study areas, which is rarely the case in monitoring applications. The sorting is mainly based on reported accuracies, taking into account the number of employed classes, in classification problems. In cases where accuracies are provided in different measures among the approaches of the same category, e.g. as a mixture of classification accuracies, root mean square errors (RMSE), R^2 values, etc., the provided sorting does not convey any comparative information. In addition, error values evaluating uncertainty of the outcomes are rarely reported within the huge set of papers reviewed for this work. However, the attempted sorting may convey useful information on the efficiency of certain sensors or algorithms for specific applications, and provide guidelines to research, monitoring, and policy-making communities.

A large number of sensors are employed in the studies discussed in the next paragraphs. Table 3 presents a list of the sensors and some of their properties as derived from the respective studies, including their spatial resolution, number of bands, cost, and their acronyms as used in the following paragraphs and the tables in the Online Resource material. Both space- and airborne sensors are listed, ranging from passive multispectral and hyperspectral to active Synthetic Aperture Radar (SAR) and Light Detection And Ranging (LiDAR). Due to their large number, airborne LiDAR sensors and digital cameras are not included in the table. Sensors with large archive of data distributed at no cost are indicated as 'free', even though new acquisitions or certain products may be commercially available. In addition, the CBD headline indicators where these sensors are involved are depicted together with a reference to an indicative high performing method (see the discussion in the next paragraphs). As a note, the CBD headline indicator on protected area monitoring is under-represented in Table 3, since several methods conducted in protected areas are discussed under other related indicators, such as ecosystem extent or species diversity.

Table 3: Acronyms and characteristics of optical multispectral/hyperspectral, SAR, and (satellite) LiDAR sensors used in CBD headline indicator extraction related studies. Abbreviations of CBD headline indicators are given in Table 1. Symbol $*$ indicates upcoming sensors, whose data have been simulated. References to a high performing method using each sensor are provided as indicative examples.

Acronym	**Sensor**	**Spatial resolution (m)**	**Bands**	**Cost**	**CBD**	**Reference**
		Optical Multispectral / Hyperspectral				
ADS40	airborne	0.2	4	yes	(1) Extent	Forzieri et al. (2013)
AHS-160	airborne	2.4	63	yes	(11) Prot. areas	Delalieux et al. (2012)
AISA	airborne (AISA Eagle)	2–2.5	272	yes	(1) Extent	Cho et al. (2012)
ALI	EO-1 ALI	30	9	free	(1) Extent, (6) Services	Chen et al. (2009)
ASTER	Terra ASTER	15, 30, 90	14	free	All	Reiche et al. (2012)
AVHRR	TIROS-N, NOAA-7, NOAA-15 AVHRR	≈1100	6	free	(1) Extent, (2) Species, (6) Services	Suarez-Seoane et al. (2002)
AVIRIS	airborne	3.5–4	224	yes	(5) Press. various	Fuentes et al. (2006)
AVNIR-2	ALOS AVNIR-2	10	4	yes	(1) Extent, (4) Press. practices	Vaglio Laurin et al. (2013)
AWIFS	IRS-P6 AWIFS	56	4	yes	(1) Extent	Sedano et al. (2013)
CAO-Alpha	airborne	0.56–1.2	24, 72	yes	(2) Species	Féret and Asner (2013)
CASI	airborne	1–3	15,36, 72	yes	(1) Extent, (2) Species, (4) Press. practices, (11) Prot. areas	Belluco et al. (2006)
DuncanTech	airborne	0.2	3	yes	(4) Press. practices	Tilling et al. (2007)

Continued on next page...

Table 3 – continued

Acronym	Sensor	Spatial resolution (m)	Bands	Cost	CBD	Reference
CHRIS	PROBA-1 CHRIS	17, 34	18, 62	free	(1) Extent	Chan et al. (2012)
DMC Z/I	airborne	2	4	yes	(4) Press. practices	Martínez-López et al. (2014)
ETM+	Landsat-7 ETM+	30	8	free	All	Griffiths et al. (2012)
GE-1	GeoEye-1	≈1–2	4	yes	(1) Extent	Newman et al. (2014)
GS	airborne (Geospatial Systems)	0.2	3	yes	(4) Press. practices	Perry et al. (2012)
HJ	HJ-1A/1B	30	4	yes	(5) Press. various	Wang et al. (2012)
HRG	SPOT-5 HRG	10, 20	4	yes	(1) Extent, (4) Press. practices	Lucas et al. (2011)
HRVIR	SPOT-4 HRVIR	10, 20	4	yes	(4) Press. practices	Soudani et al. (2006)
HYDICE	airborne	1.6	210	yes	(2) Species	Clark and Roberts (2012)
HyMap	airborne	3–5	126, 128	yes	(2) Species, (4) Press. practices	Hestir et al. (2008)
Hyperion	EO-1 Hyperion	30	220	free	(1) Extent, (2) Species, (4) Press. practices	Pu et al. (2010)
IKONOS	IKONOS	1, 4	4	yes	(1) Extent, (2) Species, (4) Press. practices	Bejarano et al. (2010)
LISS-III	IRS-P6 / IRS-1C/1D LISS-III	20–25	4	yes	(1) Extent, (4) Press. practices, (6) Services	Lucas et al. (2011)
LISS-II	IRS-1B LISS-II	36.25	4	yes	(4) Press. practices	Abbas et al. (2013)
MERIS	ENVISAT MERIS	300	15	free	(6) Services	Dente et al. (2008)
MIVIS	airborne	3	102	yes	(1) Extent	Belluco et al. (2006)
MODIS	Terra / Aqua MODIS	250, 500, 1000	36	free	All	Fang et al. (2011)
MP39	airborne (Leica MP 39)	0.25	3	yes	(4) Press. practices	Hou et al. (2011)
MSS	Landsat 1–5	60–80	4–5	free	(1) Extent	Tang et al. (2012)
OMI	Aura	13000 × 24000	740	free	(5) Press. various	Bechle et al. (2013)

Continued on next page...

Table 3 – continued

Acronym	Sensor	Spatial resolution (m)	Bands	Cost	CBD	Reference
QB	QuickBird 2	0.6, ≈2.4	4	yes	(1) Extent, (2) Species, (4) Press. practices, (6) Services	Wulder et al. (2008)
REye	RapidEye	6.5	5	yes	(4) Press. practices	Franke et al. (2012)
ROSIS	airborne	1	115	yes	(1) Extent	Belluco et al. (2006)
SeaWiFS	SeaStar SeaWiFS	1100, 4500, 9000	8	free	(2) Species, (6) Services	Zainuddin et al. (2006)
Sentinel-2*	Sentinel-2 MSI	10, 20, 60	13	free	(4) Press. practices	Herrmann et al. (2011)
SSat	SumbandilaSat	6.25	6	yes	(1) Extent	Cho et al. (2012)
TCAMP	airborne (Therma-CAMP40)	1	1	yes	(4) Press. practices	Tilling et al. (2007)
TM	Landsat-5 TM	30	7	free	All	Zhong et al. (2014)
TMI	TRMM/TMI	5000–72000	5	free	(2) Species	Zainuddin et al. (2006)
TSys	airborne (Toposys GmbH)	0.4	4	yes	(6) Services	Latifi et al. (2010)
VENμS*	VENμS VSSC	5.3	12	yes	(4) Press. practices	Herrmann et al. (2011)
VGT	SPOT–VEGETATION	1000	4	free	(2) Species	Guyon et al. (2011)
WiFS	IRS-1D WiFS	180–188	2	yes	(1) Extent	García-Gigorro and Saura (2005)
WV-2	WorldView-2	≈0.5, ≈2	8	yes	(1) Extent, (2) Species	Petrou et al. (2014)
		SAR				
ASAR	ENVISAT ASAR	30	1 (C)	free	(1) Extent, (5) Press. various, (6) Services	Mera et al. (2012)
BioSAR	airborne	30×300	1 (80–120 MHz)	yes	(4) Press. practices	Banskota et al. (2011)
ERS	ERS-1/2 AMI (SAR)	6–30	1 (C)	free	(1) Extent, (5) Press. various	Topouzelis and Psyllos (2012)
JERS-1 SAR	JERS-1 SAR	12.5–18	1 (L)	free	(1) Extent	Bwangoy et al. (2010)
PALSAR	ALOS PALSAR	≈30–50	1 (L)	yes	(1) Extent, (11) Prot. areas	Vaglio Laurin et al. (2013)
RSAT-1	RADARSAT-1	≈30–50	1 (C)	yes	(5) Press. various	Garcia-Pineda et al. (2009)
RSAT-2	RADARSAT-2	≈30–50	1 (C)	yes	(1) Extent	Evans et al. (2010)

Continued on next page...

Table 3 – continued

Acronym	Sensor	Spatial resolution (m)	Bands	Cost	CBD	Reference
SIR-C	Space Shuttle SIR-C	≈30	2 (C, L)	free	(2) Species	Bergen et al. (2007)
TDX	TanDEM-X	12	1 (X)	yes	(4) Press. practices	Kugler et al. (2014)
TSX	TerraSAR-X	18.5–40	1 (X)	yes	(4) Press. practices	Vastaranta et al. (2014)
		LiDAR				
GLAS	ICESat GLAS	70 m footprint; 172 m interval	2 (532 nm, 1064 nm)	free	(4) Press. practices, (6) Services	Nelson et al. (2009)

Figure 1 presents an overview of the RS methods reviewed in the following sections in a succinct manner. It provides information on the extracted features, the employed processing and mapping algorithms, the type of data used, and the relative performance of the method, for each particular application of the six studied CBD headline indicators. Figure 1 may serve as a guideline to detect the optimal methodology depending on the particular application, data availability, or expertise in particular algorithms. For instance, as seen from the first row of the table, synergies of active and passive sensor data and employment of supervised classification schemes (large fully coloured black triangles) usually offer high performing approaches for forest extent monitoring. As a note, studies that use features or algorithms of more than one category are represented in multiple cells. The particular characteristics of each method are analytically presented in Tables A1–A6 in the Online Resource material. The methods are indicatively sorted based on their best reported accuracies, when available. For each study, the principal sensor data are listed ('RS data'). In addition, 'Feature extraction' lists the features employed and the algorithms used for data processing, whereas 'Mapping methods' the classification and regression techniques. The final product of each method is provided, together with the best achieved accuracies.

3.1 CBD 1: Trends in extent, condition and vulnerability of ecosystems, biomes, and habitats

RS data are effectively used in various mapping applications, ranging from mixed land cover (LC) (Hansen and Loveland 2012; Xie et al. 2008) and habitat (McDermid et al. 2005) tasks, to specific target areas, e.g. forests (Wulder et al. 2012) and wetlands (Adam et al. 2009), addressing different elements of the related CBD headline indicator. Trends may be extracted by using time series of data or extracted products. Among the cited methods, several use data time series; others use single-date imagery, their expansion to studying trends being straightforward if data time series are available. Methods for LC and habitat mapping, of both terrestrial and aquatic biomes, provide direct information on their extent and condition, whereas methods for ecosystem degradation or deforestation, and fragmentation or connectivity offer valuable input to ecosystem condition and, even, vulnerability assessments.

Herein, the studies are organized under: (1) terrestrial mapping, including (1a) forests, (1b) various vegetation types, such as grasslands, savannas, heathlands, and steppes, and (1c) mixed LC and habitats; (2) ecosystem degradation and deforestation; (3) ecosystem fragmentation and connectivity; and (4) aquatic mapping, including (4a) freshwater and (4b)

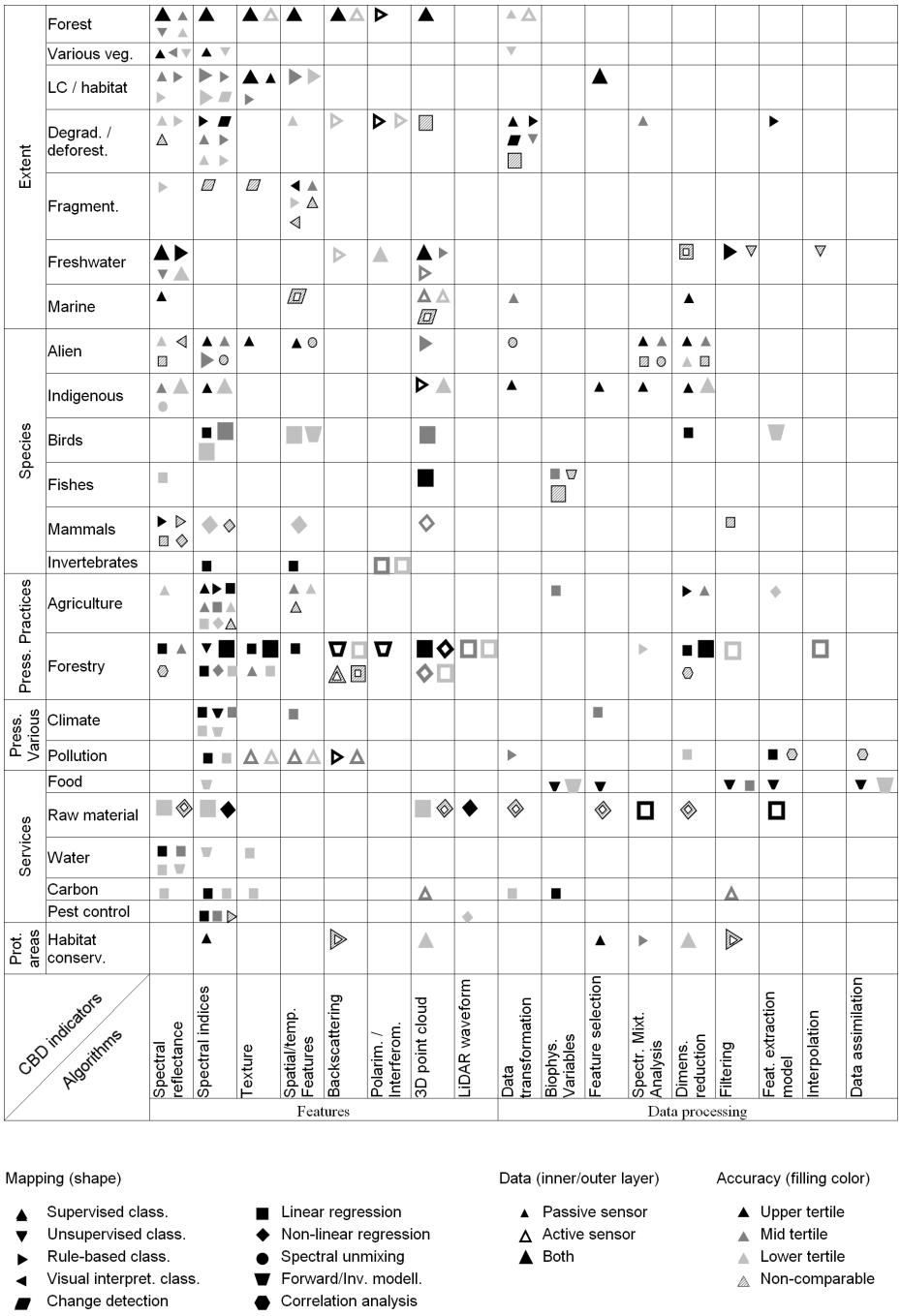

Fig. 1 Overview of remote sensing methods for the extraction of CBD headline indicators. Each symbol represents one or more methods with similar characteristics. Symbol shapes represent different mapping methods. Symbols with solely their inner, outer, or both layers coloured represent use of solely passive, active, or both passive and active data, respectively. Shape greyscale filling colours indicate method performance. Individual method details can be found in Tables A1–A6 in the Online Resource material.

marine and coastal biomes. The methods described below, succinctly presented in Figure 1 and analytically in Table A1 of the Online Resource, can be employed to monitor progress to Aichi target 5 (Table 1), on the reduction of habitat loss, fragmentation, and degradation.

3.1.1 Terrestrial mapping

Landsat data, including the Multispectral Scanner (MSS), Thematic Mapper (TM), and Enhanced Thematic Mapper Plus (ETM+) sensors, are effective sources for terrestrial mapping, including habitat classification (Boyd et al. 2006; Bock et al. 2005), LC mapping of tropical areas (Paneque-Gálvez et al. 2013), savannas (Sano et al. 2010), grasslands (Price et al. 2002), or forests (Jiang et al. 2004; Wijedasa et al. 2012), and change detection (Demir et al. 2013; Berberoglu and Akin 2009). Other optical data include: the similar spatial resolution (i) Advanced Spaceborne Thermal Emission and Reflection Radiometer (ASTER) (Reiche et al. 2012; Lucas et al. 2011) and (ii) Linear Imaging Self Scanning Sensor 3 (LISS-III) (Lucas et al. 2011); the higher resolution (iii) Advanced Visible and Near Infrared Radiometer type 2 (AVNIR-2) (Vaglio Laurin et al. 2013) and (iv) High Resolution Geometric (HRG) instrument (Lucas et al. 2011); and the very high resolution (VHR) (v) QuickBird and (vi) WorldView-2 (Petrou et al. 2014; Adamo et al. 2014) sensors. Although of lower spatial resolution, data time series from the Moderate Resolution Imaging Spectroradiometer (MODIS) have proven successful in mapping dry savanna vegetation, capturing phenological properties with inter-annual classification average user's and producer's accuracies reaching 94.86% and 97.73% for 12 classes, respectively (Hüttich et al. 2009). Hyperspectral data features have shown high potential in discriminating vegetation types (Forzieri et al. 2013; Vyas et al. 2011; Chan et al. 2012). Furthermore, besides their ability in providing vegetation structure information, as discussed in next paragraphs, active data have been increasingly used in mapping applications. Phased Array type L-band SAR (PALSAR) and RADARSAT-2 data have provided high potential in LC and forest characterization, used either individually (Walker et al. 2010; Maghsoudi et al. 2012; Longépé et al. 2011) or in synergy with optical data (Liesenberg and Gloaguen 2013; Vaglio Laurin et al. 2013). In a study by Vaglio Laurin et al. (2013), PALSAR coupled with AVNIR-2 identified eight LC classes in a tropical rainforest and fragmented area with accuracy 97.5%, outperforming PALSAR synergy with Landsat TM. In addition, Airborne Laser Scanning (ALS), i.e. airborne LiDAR, data proved particularly effective in forest delineation in upper timberline and fragmented forests in Austria, reaching 96% detection accuracy (Eysn et al. 2012).

Mapping is performed through various classification approaches, including both knowledge (Lucas et al. 2015; Pérez-Luque et al. 2015; Petrou et al. 2014; Adamo et al. 2014) and data driven (Paneque-Gálvez et al. 2013; Forzieri et al. 2013; Chan et al. 2012) ones. The former provide the flexibility to incorporate expert knowledge in the classifier and achieve rational classification results even in special cases or classes not included in the particular training site, although with the expense of labour and time consuming trial-and-error rule fine-tuning. Conversely, data driven approaches can offer fast automated classifier training, even in cases of multivariate data. However, classifiers in this category, mainly the supervised ones, are restricted to the classes present in the training site and fail to identify unknown classes in different test sites. Adamo et al. (2014) developed a knowledge driven algorithm based on a variety of spectral, topological, and texture features from multitemporal QuickBird, WorldView-2 and LiDAR data to map Annex I habitats and General Habitat Categories (GHC). Petrou et al. (2014) expanded this approach, developing a fuzzy evidential reasoning classifier to handle uncertainty from noise afflicted data and inaccurate expert rules. On data driven approaches, apart from cases proposing new classification and change

detection schemes (Demir et al. 2013; Jiang et al. 2004), most studies have employed widely used, mainly supervised, classifiers. Support Vector Machines (SVM) are among the most widely used and highly performing ones. In a Natura 2000 heathland characterization study (Chan et al. 2012), SVM outperformed Random Forest (RF) and AdaBoost tree ensemble classifiers by around 4.5% in experiments involving 18 features from a hyperspectral image for 537 samples in 10 classes. Interestingly, using three times more features, the performance of RF and AdaBoost reached the one of SVM, whereas the latter remained the same; this indicated that SVM classifier was more sensitive to the Hughes phenomenon, resulting in decrease of classifier performance when the number of features is high compared with the number of training samples (Chi et al. 2008). In other studies, SVM outperformed *k*-nearest neighbour (*k*-NN), binary Classification And Regression Tree (CART), and Maximum Likelihood Classifier (MLC) (Paneque-Gálvez et al. 2013; Boyd et al. 2006). The latter has outperformed Spectral Angle Mapper (SAM) and Spectral Information Divergence (SID) classifiers in a study by Forzieri et al. (2013). Artificial Neural Networks (ANN) have shown advantages over SVM, SAM, or MLC in different studies (Vaglio Laurin et al. 2013; Vyas et al. 2011). It is worth noting, though, that ANN implementation proved incapable to build a model when 165 features were employed by Vyas et al. (2011), probably due to the very complicated resulting network of nodes; on the contrary, SVM and SAM classifiers could handle this size of feature sets and perform the classification. Overall, the existence of a universally best performing classifier in all mapping tasks is highly unlikely, making research on high performing generic or task oriented classifiers an ongoing process.

Object-based image analysis (OBIA) and classification approaches gain space over pixel based ones (Blaschke 2010; Blaschke et al. 2008; Manakos et al. 2000), mainly in applications using VHR data (with spatial resolution finer than 3 m), e.g. habitat mapping (Adamo et al. 2014, 2013; Lucas et al. 2011). However, object-based classification has proven more effective than pixel based also in some cases where coarser resolution data were used, e.g. the delineation of forest clear cuts with Landsat data, using spectral features, polygon shape parameters, and context with other classes (Flanders et al. 2003). In general, multiple reasons favour the use of object-based analysis over pixel-based approaches, particularly for mapping applications. The large spectral variabilities within habitats may create inaccurate classifications and salt-and-pepper effects under pixel-based approaches for VHR images, proving them inappropriate for habitat classification (Zohmann et al. 2013; Kobler et al. 2006; Bock et al. 2005). Furthermore, pixel-based approaches prohibit the extraction of spatial, contextual, and topological features, such as object area or adjacency to other objects of specific class, that are valuable for certain classification tasks (Petrou et al. 2014).

3.1.2 Degradation / deforestation

Satellite data are considered as the only realistic means to monitor deforestation and forest degradation at a timely manner (Lynch et al. 2013). Data time series are necessary to detect deforestation. Landsat data have been primarily used in monitoring forest disturbance (Griffiths et al. 2012; Schroeder et al. 2011; Zhu et al. 2012; Grinand et al. 2013; Huang et al. 2010; Gorsevski et al. 2012; Renó et al. 2011; Goodwin and Collett 2014), mainly due to the long archive, spectral and spatial resolution properties, and the free availability of data. Tasseled Cap Transformation (TCT) indices from Landsat near-annual time series, evaluated under trajectory-based change detection methods, resulted in identifying forest disturbances within 22 years with overall accuracy (OA) 95.72% (Griffiths et al. 2012). The Continuous Monitoring of Forest Disturbance Algorithm (CMFDA) has taken advantage of the full Landsat archive of an area to timely detect forest disturbances, by even predicting

unseen Landsat pixel reflectance values (Zhu et al. 2012). Although highly accurate disturbance maps may be extracted, a period of more than one month is required to confidently detect changes, expected to be more in areas with low Landsat imagery coverage. Thus, fusion with similar sensors that have shown consistent results, e.g. HRG (Lück-Vogel et al. 2013), or sensors with higher temporal resolution is expected to be crucial for global near-real time deforestation monitoring. Other employed data include the passive Advanced Very High Resolution Radiometer (AVHRR) (Dubinin et al. 2010), Advanced Wide Field Sensor (AWiFS), and MODIS (Sedano et al. 2013) sensors, as well as active PALSAR time series (Motohka et al. 2014; Whittle et al. 2012). The latter, providing the ability of cloud unobstructed monitoring, can have comparative advantages in highly cloud covered areas, such as tropical rainforests. Wider availability of free satellite data, at least from government agencies, should be a policy-makers' priority (Turner 2013).

3.1.3 Fragmentation / connectivity

Fragmentation and connectivity can affect biodiversity significantly, isolating living species areas and allowing the invasion of alien or destructive species, respectively. Despite the common notion, Fahrig (2003) argued that fragmentation per se may affect biodiversity also positively and should be distinguished by habitat loss, whereas Kindlmann and Burel (2008) suggested that connectivity should be assessed both in landscape and organism (functional) diversion, allowing different degrees of connectivity for different species within a landscape.

Numerous landscape measures are proposed to assess fragmentation and connectivity, at the patch or landscape level, whose estimation is based on LC or habitat map monitoring, or change assessment. FRAGSTATS software measures (McGarigal et al. 2012) are widely adopted for fragmentation, estimated using Landsat (Tang et al. 2012; Wang et al. 2011; Liu et al. 2014; Virtanen and Ek 2014; García-Gigorro and Saura 2005), IKONOS-2, GeoEye-1 (Newman et al. 2014), QuickBird, ASTER (Virtanen and Ek 2014), or Wide Field Sensor (WiFS) (García-Gigorro and Saura 2005) imagery. Variogram analysis is also employed to assess forest heterogeneity (Cho et al. 2012). In addition, a number of indices are used to assess connectivity, e.g. in forested areas, including the Integral Index of Connectivity (IIC) (Liu et al. 2014) or the Equivalent Connected Area Index (Martín-Martín et al. 2013).

Direct comparison on the efficiency of the measures describing the degree of fragmentation or connectivity is not straightforward (Goodwin 2003). Various criteria are suggested by Saura and Pascual-Hortal (2007), where the proposed Probability of Connectivity index is acknowledged as the only satisfying all defined requirements. Plexida et al. (2014) identified Patch Density, Area-Weighted Mean Fractal Dimension Index, and Patch Cohesion Index as the most suitable measures to describe landscape patterns in different scales. García-Gigorro and Saura (2005) evaluated the sensitivity to scale of various fragmentation indices.

3.1.4 Aquatic mapping

Airborne LiDAR is extensively used in aquatic area mapping, due to the ability of its point cloud or full waveform to extract accurate Digital Elevation Models (DEM). Lang and McCarty (2009) distinguished wetland inundation below the forest canopy from non-inundated and transitional areas with overall accuracy up to 96.3%. Other applications include upland swamp boundary detection (Jenkins and Frazier 2010), and river (Höfle and Vetter 2009) or tidal (Brzank et al. 2008a,b; Schmidt and Soergel 2013) water mapping. In addition, L-band and C-band SAR data are effectively used in wetland and mangrove characterization (Bwangoy et al. 2010; Evans et al. 2010; Lang et al. 2008; Kumar and Patnaik 2013).

On passive sensors, Belluco et al. (2006) evaluated a range of multispectral and hyperspectral ones, namely the airborne Reflective Optics System Imaging Spectrometer (ROSIS), Compact Airborne Spectrographic Imager (CASI), and Multispectral Infrared and Visible Imaging Spectrometer (MOVIS), and the satellite QuickBird and IKONOS-2, in salt-marsh vegetation mapping. Hyperspectral ROSIS and CASI slightly outperformed the multispectral ones, whereas MLC the SAM and K-means classifiers consistently. Minimum Noise Fraction (MinNF) and band averaging outperformed Principal Component Analysis (PCA) in feature dimensionality reduction. In Pu et al. (2010), hyperspectral Hyperion data surpassed the same or higher spatial resolution data of Advanced Land Imager (ALI), Landsat TM, and IKONOS in seagrass habitat mapping. Both studies confirmed the advantages of dense spectral information for wetland mapping, with the former highlighting the even greater importance of high spatial resolution (HR) data. Thus, future HR hyperspectral satellite sensors, beside the only existing coarser resolution Hyperion, would highly benefit timely wetland monitoring. Airborne optical cameras have been used for upland swamp (Lechner et al. 2012) and wetland (Mwita et al. 2013) mapping, coarser resolution Landsat data being insufficient if used alone, for the latter application. Super-resolution techniques have been proposed to improve mapping by increasing the spatial resolution of satellite images, while preserving their spectral properties, e.g. in representation of lakes using data time series, halftoning, and morphological filtering (Muad and Foody 2012). Approaches based on discrete wavelet transform for hyperspectral images (Patel and Joshi 2015) and structural self-similarity, identifying similar structures in RS images (Pan et al. 2013), have been recently proposed. Assuming the existence of co-registered images of different spatial and spectral resolutions, Atkinson et al. (2008) used downscaling cokriging for image mapping, whereas Song et al. (2015) avoided the restriction for co-registration through an image degradation model via blurring and downsampling and deriving a simulated medium resolution image from a high resolution one; the former was then used to extract a dictionary employed to increase the resolution of the originally targeted medium resolution image.

3.2 CBD 2: Trends in abundance, distribution, and extinction risk of species

Abundance and distribution of species constitute a core part of biodiversity. The respective CBD headline indicator encompasses both plant and animal species. A number of recent studies are reviewed, successfully employing RS data to study species distribution and abundance, either through direct monitoring or through proxy variables. The methods are organized under: (1) plant species, including (1a) alien and (1b) indigenous species; and (2) animals, including (2a) birds, (2b) fishes, (2c) mammals, and (2d) invertebrates. The methods are connected to Aichi targets 9 and 12 (Table 1), on monitoring invasive and threatened species, respectively. Additional details are listed in Table A2 in the Online Resource.

3.2.1 Plant species

The spatial resolution of the remote sensor is crucial in species monitoring (Joshi et al. 2004). As rule of thumb, the optimal spatial resolution of the sensor is suggested to be two to five times smaller—i.e. finer—than the monitored object, to provide an effective trade-off between within-object and between-object variance (Nagendra 2001). Some of the best performing studies in alien and invasive species detection are based on fine resolution data, either aerial (Dorigo et al. 2012; Shouse et al. 2013; Artigas and Pechmann 2010; Hantson et al. 2012; Clark and Roberts 2012; Colgan et al. 2012) or satellite (Laba et al. 2008; Walsh

et al. 2008; Immitzer et al. 2012). Dorigo et al. (2012) extracted a bi-temporal band ratio (BTBR) and a number of Haralick texture features from bi-seasonal digital orthophotos and successfully detected *Fallopia japonica*, one of the world's worst invasive alien species, with up to 90.3% PA and 98.1% UA. Similar results were achieved neglecting the near infrared (NIR) band one of the photos had, suggesting the transferability of the method to cases where only true colour photos are available.

Similar to vegetation and wetland mapping, hyperspectral data perform high in species mapping and plant invasion applications during the last years (He et al. 2011), especially in areas of high habitat and species diversity (Nagendra et al. 2013), and are widely employed (Clark and Roberts 2012; Artigas and Pechmann 2010; Féret and Asner 2013; Colgan et al. 2012; Hestir et al. 2008; Baldeck et al. 2014; Ghiyamat et al. 2013; Pengra et al. 2007; Miao et al. 2006; Somers and Asner 2012). Thenkabail et al. (2004) demonstrated the use of hyperspectral data by simulating the bands of Hyperion with a hand-held spectroradiometer to discriminate vegetation and agricultural crops. Use of PCA, lambda-lambda R^2 models, stepwise discriminant analysis (SDA), and derivative greenness vegetation indices (DGVI), identified 22 optimal bands that resulted in classification of five weed species with 97% OA. Despite their high utility, the application of hyperspectral data may be limited by the restricted availability of satellite data and the necessity of aerial surveys. Satellite data from Hyperion, although having shown better discrimination ability than multispectral or VHR sensors (Pu et al. 2010), have limited spatial resolution compared with aerial surveys. Technical challenges by the large amount of data are expected to be reduced with the increasing research on feature selection and dimensionality reduction approaches.

Féret and Asner (2013) evaluated parametric and non-parametric classifiers, including SVM, ANN, *k*-NN, and Linear (LDA), Quadratic (QDA), and Regularized Discriminant Analysis (RDA), in tropical tree species discrimination; RDA achieved the best performance with small training sample sets, whereas SVM with larger ones. Object-based classification outperformed pixel-based, with both providing inferior accuracies to majority-class rule classification, where an object is classified to the class where the majority of its pixels are classified. Artigas and Pechmann (2010) applied MinNF and SAM on airborne hyperspectral data and digital photos, to successfully map invasive *Phragmites australis* with 93% PA and 96% UA. Among other sensors, ALS data have shown high potential in discriminating wetland vegetation species (Zlinszky et al. 2012).

3.2.2 Animal species

Whereas monitoring the distribution and abundance of animal species is crucial for biodiversity assessment and species interrelations, e.g. with invasive animal species (EEA 2012a), direct observation is rarely possible and mainly restricted in large mammals with the use of VHR sensors. As an example, WorldView-2 data, and particularly a thresholding classifier using the Coastal band (400–450 nm), detected whales with up to 84.6% PA and 76.3% UA (Fretwell et al. 2014). Instead, the most common way to estimate distribution of animal species, including mammals, birds, fishes, or invertebrates, is to model it based on proxies, such as spectral or structural properties (Suarez-Seoane et al. 2002; Buchanan et al. 2005; Vogeler et al. 2014; Bejarano et al. 2010; Mairota et al. 2015), habitat suitability (Duro et al. 2014; Yen et al. 2012; Melin et al. 2013), or detection of colonies (Fretwell and Trathan 2009; Fretwell et al. 2012).

Suarez-Seoane et al. (2002) combined AVHRR with topographic and Geographic Information System (GIS) data to model the occurrence of three agricultural steppe birds in

Spain, using PCA and Generalized Additive Models (GAM). Other studies included Landsat imagery, either individually (Buchanan et al. 2005; Duro et al. 2014) or in synergy with SAR data (Bergen et al. 2007), to derive forest parameters and relate them with species distribution through linear regression. The fusion of LiDAR structure variables with spectral information appears beneficial for avian species distribution assessment (Vogeler et al. 2014; Clawges et al. 2008). Based on the notion that the 3D structure of coral reef fish habitat intensely affects their communities, acoustic data have been used in synergy with VHR IKONOS-2 to correlate abundance of species with habitat characterization and topographic features, using regression and Negative Binomial General Linear Models (NBGLM) (Bejarano et al. 2010; Purkis et al. 2008). Airborne LiDAR data have also been used to model the presence of invertebrates spider (Vierling et al. 2011) and beetle (Müller and Brandl 2009), using Constrained Redundancy Analysis (CRA), and Canonical Correlation Analysis (CCA) and Multiple Linear Regression Models (MLRM), respectively. Other passive data, such as MODIS (Kumar et al. 2009; Yen et al. 2012), VEGETATION (Pittiglio et al. 2012), Landsat (Arias-González et al. 2011; Koy et al. 2005), or Tropical Rainfall Measuring Mission's Microwave Imager (TRMM/TMI) and Sea-Viewing Wide Field-of-View Sensor (SeaWiFS) (Zainuddin et al. 2006) have been used in different animal abundance modelling studies with satisfactory accuracies, employing mainly a plethora of regression techniques.

3.3 CBD 4: Trends in pressures from unsustainable agriculture, forestry, fisheries, and aquaculture

Pressures from unsustainable management in agricultural, forest, and aquatic areas can be inferred up to a degree by RS methods. Most studies focus on forestry applications, mainly on biomass and forest structural parameters, supporting United Nations (UN) Reducing Emissions from Deforestation and Forest Degradation (REDD+) activities (Langner et al. 2012), whereas pressures from unsustainable agriculture can be inferred mainly from changes in Land Use (LU), irrigation strategies, or nitrogen concentration. Pressures from unsustainable fisheries and aquaculture through RS have not been extensively studied per se, but can be deduced up to a degree by monitoring fish distribution and abundance, or pollution in aquatic areas. Several high performing methodologies that can be used to monitor agriculture and forestry management unsustainable practices and serve monitoring of Aichi targets 4, 5, 6, and 7 (Table 1) are discussed below and analytically listed in Table A3.

3.3.1 Agriculture monitoring

Studies revealing pressures from unsustainable agriculture practices have mainly focused on effects from irrigation strategies (Abbas et al. 2013; Martínez-López et al. 2014; Shahriar Pervez et al. 2014), nitrogen treatment (Tilling et al. 2007; Chen et al. 2010; Perry et al. 2012), and crop characterization (Zhong et al. 2014; Alcantara et al. 2012; Jain et al. 2013). Structural properties of the studied areas are less revealing than spectral ones for these tasks, therefore passive multispectral or hyperspectral data have mainly been used.

LISS-II time series have been useful in extracting ground salinity indices (Abbas et al. 2013). Following the LU mapping of the study area, salinity affected soils of different degree were identified as crucial tool for irrigation management. The forthcoming superspectral VENμS and Sentinel-2 sensors, simulated by a field spectrometer, have been evaluated by Herrmann et al. (2011) in estimating Leaf Area Index (LAI) of wheat and potato crops. Both sensors were found promising in performing as well as a hyperspectral sensor, whereas the

calculated Red-Edge Inflection Point (REIP) index, using their four red-edge bands, was proven more consistent than the Normalized Difference Vegetation Index (NDVI).

Multispectral data with large extent coverage and high revisit time have been preferred in crop area characterization. Different methodologies employing Landsat TM/ETM+ and MODIS data have been evaluated in cropping intensity mapping in smallholder farms, in different spatial scales (Jain et al. 2013). Thresholding Landsat-derived NDVI values outperformed three MODIS based methodologies in almost all scales for both winter and summer periods, with hierarchical training method being the best among the MODIS ones. Zhong et al. (2014) showed that phenological metrics extracted by TM/ETM+ time series can map corn and soybean more accurately than spectral features in cross-year classifications, i.e. when the training and test features correspond to different cropping years. Mapping of abandoned agriculture has also been feasible by MODIS time series (Alcantara et al. 2012).

3.3.2 Forestry monitoring

Structure-based indicators have been suggested as core elements for sustainable forest management (Lindenmayer et al. 2000). Active sensors, including mainly LiDAR, have been proven the most effective sources of forest structure information (Lindberg and Hollaus 2012; Hyyppä et al. 2012; Koch 2010). Besides the usually employed first pulse and statistical point height metrics, last pulse and individual tree-based features have shown increased accuracy in approximating tree height, density at breast height, and stem volume in a boreal managed forest (Hyyppä et al. 2012). However, although the omission errors in tree detection are reduced, the commission errors are increased; therefore, a synergy of first and last pulse data might combine the benefits of the former in detecting non-overlapping trees and of the latter in overlapping ones. Besides satellite LiDAR data (Duncanson et al. 2010; Wang et al. 2014), the synergy of TanDEM-X and TerraSAR-X, as the first source of spaceborne single-pass polarimetric SAR interferometry (PolInSAR) data, has been proven particularly promising for future height estimation applications. Kugler et al. (2014) evaluated single polarization data with ancillary DTM and reached correlations with LiDAR derived height up to $R^2 = 0.98$, while using solely dual polarization data resulted in $R^2 = 0.86$. In general, as rule of thumb, 25–30 m SAR spatial resolution or 25 m LiDAR footprint diameter are required to capture vegetation structure for biodiversity application (Bergen et al. 2009). Other promising alternatives to active sensor data have included multispectral or hyperspectral data, mainly using neighbourhood statistics, spectral indices, or texture features (Wolter et al. 2009; Kayitakire et al. 2006; Cho et al. 2009; White et al. 2010; Petrou et al. 2012).

Although LiDAR data are effective in vertical forest structure characterization, their repeated applicability is limited by high costs (Wolter et al. 2009), technical challenges (Nagendra et al. 2013), and restricted understanding on interactions between LiDAR beams and vegetation (Koch 2010). High costs are mainly related to the need for airborne campaigns, since satellite LiDAR data are limited. Upcoming missions, such as the Ice Cloud and land Elevation Satellite II (ICESat II) and Deformation, Ecosystem Structure and Dynamics of Ice (DESDynI) missions (Popescu et al. 2011), are expected to provide lower cost coverage with similar performance to aerial surveys. Further training of ecologists and site managers on the use of LiDAR data, and further research on beam properties and interactions with, especially multi-layer, vegetation are expected to favour wider applicability. Furthermore, SAR data in vegetation structure studies have been mainly restricted by temporal decorrelation limitations, especially in high biomass forests (Koch 2010). Missions such as the Tandem-X and TerraSAR-X platforms, in synergy forming a single-pass polarimetric interferometer, are expected to counteract temporal decorrelation; in addition, new missions, e.g.

Sentinel-1, started to provide free high resolution data for further applications. Synergies of LiDAR/SAR data remain a promising field for future research (Bergen et al. 2009).

Additional parameters assessing forest sustainability have been measured by RS studies. Nichol and Sarker (2011) recently presented a study where texture feature ratios extracted from AVNIR-2 and HRG data were successfully employed in modelling biomass with R^2 up to 0.939. LiDAR, SAR, and even Landsat data have been also employed in biomass estimation studies (Kronseder et al. 2012; Banskota et al. 2011; Vastaranta et al. 2014; Langner et al. 2012; Sandberg et al. 2011). Stem volume and basal area have been estimated through a synergy of ALS with airborne colour infrared (CIR) and AVNIR-2 data (Hou et al. 2011). Ozdemir and Karnieli (2011) have used WorldView-2 data and texture analysis to approximate a number of additional parameters, including Standard Deviation of Diameters at Breast Heights (SDDBH), Gini Coefficient (GC), and Diameter Differentiation Index (DDI). ETM+ data have outperformed the higher spatial resolution but lower spectral information IKONOS and SPOT-4 High-Resolution Visible and Infrared sensor (HRVIR) in LAI estimation (Soudani et al. 2006), with ALS data being reported as alternatives (Zhao and Popescu 2009). Finally, managed forest disturbances, due to logging activities, have been monitored with Landsat time series (Kuemmerle et al. 2009), whereas RapidEye VHR imagery has been used in logging trail detection (Franke et al. 2012).

3.4 CBD 5: Trends in pressures from habitat conversion, pollution, invasive species, and climate change

Habitat mapping and conversion from one category to another has been extensively studied and pressures may be inferred from methods discussed in Section 3.1. Furthermore, numerous studies on species invasion detection and respective pressures have successfully employed RS data (Section 3.2). This paragraph focuses on the potential detection of pressures from climate change and pollution. Table A4 lists recent state-of-the-art methodologies, related to the monitoring mainly of Aichi targets 4, 5, 8, 9, and 10 (Table 1).

Climate change severely affects biodiversity at different scales and may influence species phenology, physiology, or range (Bellard et al. 2012). RS data offer high potential in monitoring species range, extent, and distribution, as mentioned in previous sections, whereas the task of assessing physiological changes and adaptivity to new conditions seems more challenging. SPOT-4 and SPOT-5 VEGETATION data time series have been effective in detecting variations in leaf phenology of deciduous broadleaved forest in different elevations, extracting a five year perpendicular vegetation index (PVI) and using a temporal unmixing method (Guyon et al. 2011). A number of indices from MODIS or Landsat data, including Enhanced Vegetation Index (EVI), NDVI, Excess Green Index (ExG_M), and Normalized Difference Water Index (NDWI), were evaluated in several studies (Hmimina et al. 2013; Hufkens et al. 2012; White et al. 2014). The optimized soil-adjusted vegetation index (OSAVI), calculated from MODIS data, was more consistent than NDVI and EVI in characterizing Gross Primary Productivity (GPP) end in evergreen needleleaved forests, encouraging its broader use (Wu et al. 2014). In general, phenology monitoring in deciduous broadleaved forests seems more feasible than needleleaved forests or savannas. Correlation of RS estimates with systematic field observations of phenology of multi-layer canopy is expected to further improve relevant RS derived land surface models (Ryu et al. 2014).

Detection of various pollution sources is feasible, up to one degree, by RS methods. Oil spills have been widely monitored, although RS data seem to only complement rather than fully replace airborne observations, due to the particularities of oil spills (Leifer et al.

2012). SAR data are mainly used to detect oil spills in oceans, because of their all weather and illumination condition monitoring, wide coverage, and the ability to separate oil from surrounding water area, under low or moderate wind (Fingas and Brown 2014), where oil surface appears significantly smoother. Mera et al. (2012) used ENVISAT Advanced SAR (ASAR) data with an Adaptive thresholding algorithm to almost perfectly label oil spill pixels in Iberian Peninsula. Other studies employed C-band RADARSAT-1 (Garcia-Pineda et al. 2009) and European Remote Sensing Satellite 2 (ERS-2) SAR data (Topouzelis and Psyllos 2012), as well as airborne hyperspectral Airborne Visible / Infrared Imaging Spectrometer (AVIRIS) data (Kokaly et al. 2013). In addition, studies have been conducted to detect non-point source pollution, identified as a core arising issue in water environmental protection (Shen et al. 2012), such as total nitrogen, total phosphorous, ammonia nitrogen (NH_4-N) and chemical oxygen demand (CODcr) with multispectral HJ-1A and HJ-1B data (Wang et al. 2012). Furthermore, ozone injury to coniferous forest (Kefauver et al. 2013) and urban ground-level nitrogen dioxide (NO_2) (Bechle et al. 2013) have been assessed using Ozone Monitoring Instrument (OMI) and airborne hyperspectral data, respectively.

3.5 CBD 6: Trends in distribution, condition, and sustainability of ecosystem services for equitable human well-being

Ecosystem services declined significantly during the last years (Costanza et al. 2014), and the need for sustainable management is prominent. The usual categorizations of ecosystem services include the Millennium Ecosystem Assessment (MA), The Economics of Ecosystem and Biodiversity (TEEB), and the Common International Classification of Ecosystem Services (CICES) classifications (Maes et al. 2013). MA identifies four categories: provisioning (e.g. food, raw materials, water), regulating (e.g. carbon storage, pest control), cultural (e.g. tourism), and supporting services (e.g. soil formation). The latter was considered a subset of ecological processes by TEEB and replaced by habitat services (e.g. maintenance of genetic diversity), whereas CICES is based on MA and TEEB classifications, focusing more on ecosystem (capital) accounts and following a hierarchical structure (Maes et al. 2013). Habitat services, as discussed in previous sections, are assessed mainly through their presence and condition, whereas cultural services are relatively more challenging to be monitored by RS data. Provisioning and regulating services, the focus of this section, have attracted wide interest by the research community (Ayanu et al. 2012), their assessment with RS data being promising yet challenging. The discussed methods are mainly relevant with the Aichi targets 14 and 15 (Table 1), on monitoring ecosystem services and resilience, respectively. Table A5 provides further details on the methods.

3.5.1 Provisioning services

Studies on food, raw material, and water provisioning services use a variety of data. Through data assimilation, the MODIS LAI product and extracted vegetation indices of NDVI and EVI forecast crop yield, using only a partial year of data, with relative deviations from reference data less than 3.5% (Fang et al. 2011). Passive MODIS, AVHRR, and Medium Resolution Imaging Spectrometer (MERIS), and active ASAR data, have been used to estimate wheat or maize yield with relative differences less than 11% (Moriondo et al. 2007; Ren et al. 2008; Yan et al. 2009; Dente et al. 2008). Furthermore, LiDAR data, either airborne (Jaskierniak et al. 2011; Tonolli et al. 2011; Latifi et al. 2010) or spaceborne (Nelson et al. 2009), have been the primary sources to estimate timber volume. Jaskierniak et al.

(2011) used mixture models with distributions based on GAM for Location, Scale and Shape (GAMLSS) with airborne LiDAR data, to correlate observed stand volume and basal area values in a eucalyptus native forest with $R^2 = 0.88$ and $R^2 = 0.89$, respectively.

Mainly passive sensors are employed to assess water quality, clarity, and turbidity in related studies, including Landsat (Olmanson et al. 2008; Zhao et al. 2011; Kabbara et al. 2008), Earth Observing 1 (EO-1) Advanced Land Imager (ALI) (Chen et al. 2009), and SeaWiFS (Chen et al. 2007). As a characteristic example, a 20-year archive of Landsat data was effective in providing correlations with field-measured Secchi Disk Depths (SDD) up to $R^2 = 0.96$, to characterize water clarity in Minnesota lakes, USA (Olmanson et al. 2008).

3.5.2 Regulating services

Hyperspectral Airborne Visible Infrared Imaging Spectrometer (AVIRIS) data have been used for the derivation of NDVI, Photochemical Reflectance Index (PRI), and water content indices, and the extraction of carbon and water flux maps in a semi-arid area (Fuentes et al. 2006). Regression analysis resulted in adjusted R^2 values up to 0.96 and 0.94 for net carbon and water fluxes, respectively. Airborne LiDAR (García et al. 2010) and QuickBird and ASTER spectral, texture, and transformation features (Fuchs et al. 2009) have also been used to assess carbon stocks. Regarding pest control, several studies detected defoliation and other effects and may be used to infer the resistance of a study area to pest attack. Multispectral or hyperspectral data have mainly been employed to detect affected areas. Time series of VHR multispectral or panchromatic data have been successful in evaluating pine beetle red attack over time (Wulder et al. 2008); QuickBird time series and extracted red-to-green band ratios lead to true positive accuracies of 89–93% for three studied years. Spectral properties of MODIS, AVIRIS, and Landsat data, together with regression analysis, have assessed gypsy moth defoliation (Debeurs and Townsend 2008), decline in emerald ash borer-infested areas (Pontius et al. 2008), and mortality of lodgepole pine to bark beetle attack (Coops et al. 2009).

3.6 CBD 11: Trends in coverage, condition, representativeness, and effectiveness of protected areas and other area-based approaches

Around 133,000 protected areas exist worldwide, increased by 400% since the 1970's and covering approximately 13.9% and 3.2% of the terrestrial and marine environment, respectively (Kachelriess et al. 2014; Nagendra et al. 2013; Butchart et al. 2010). Although delineation of protected areas indicates the conservation status, these statistics per se can poorly describe the condition within the protected areas and the effectiveness of the conservation management practices (Nagendra et al. 2013). RS data can assist monitoring of both the protected sites and their surrounding areas, since the condition, changes, and pressures of the latter closely or equally affect the former (Laurance et al. 2012). Different parameters may well be assessed by RS methods discussed in previous sections, e.g. LC or habitat extent, fragmentation, and degradation (Section 3.1), species invasion or distribution and abundance (Section 3.2), or pressures from unsustainable forestry (Section 3.3), with the additional potential requirement of higher temporal coverage for timely monitoring. This section focuses on methods for conservation assessment guidelines, as indicative examples on how RS can address needs of the related CBD headline indicator. Methods reported in this and previous sections, are linked mainly to the related Aichi targets 11, 14, and 15, as noted in Table 1. Method details can be found in Table A6.

ASTER vegetation indices in synergy with species richness and topographic and climatic variables characterized vegetation structure and model the spatial variation in woody species richness in a protected temperate forest in Chile (Altamirano et al. 2010). Developed models predicted future tree species richness, identified gaps in current conservation strategies, and suggested the creation of new protected areas. Using Multiple Endmember Spectral Mixture Analysis (MESMA) in Airborne Hyperspectral line-Scanner radiometer (AHS-160) data, Delalieux et al. (2012) delineated three heather age classes in a Natura 2000 site with OA around 86%, assisting conservation management of natural heathlands. Airborne multispectral CASI and LiDAR data have mapped protected cork oak forests and characterized habitat condition as high, medium, and low (Simonson et al. 2013). SAR data have also shown potential in conservation planning. TerraSAR-X time series identified swath events in protected semi-natural grasslands within 11-day intervals (Schuster et al. 2011), whereas changes in PALSAR backscatter data mapped coastline retreat and health degradation in a large mangrove forest (Cornforth et al. 2013).

4 Conclusions and future considerations

The range of methods and data presented demonstrate the potential of remote sensing in biodiversity monitoring. These methods are linked to the respective CBD headline indicators, indicating methodologies that can be adopted for the constant monitoring of the progress towards the Aichi targets. Such linkage has rarely been attempted in the past and intends to reduce the gap of information sharing between the RS and the ecology, conservation biology, site manager, and policy making communities, identified also by previous studies (Kachelriess et al. 2014; Nagendra et al. 2013; Vanden Borre et al. 2011).

Despite the wide availability of RS data, they have not yet been fully exploited in operational tasks (Pettorelli et al. 2014), mainly because of the technical challenges in handling by non-experts. Thus, a more effective two-way know-how exchange between the related communities is required to fundamentally assist timely and large area biodiversity monitoring. An additional burden to wider data utilization remains the cost of certain RS products, including mainly airborne or VHR satellite ones. Free provision of RS data (Turner 2013; Blonda et al. 2013) and more systematic use of already free ones, e.g. Landsat, EO-1 Hyperion, and the upcoming Sentinels, is expected to boost the use of data and improve monitoring. Furthermore, the lack of error values evaluating uncertainty of the outcomes in the vast majority of studies in the literature is a critical issue that often prevents stakeholders to trust RS data and techniques for conservation assessment. Finally, lack of standardization for each indicator (Secades et al. 2014) restricts closer connection between user requirements and RS potential and the adoption of widely adopted robust methodologies for indicator extraction. The creation of a large scale database of RS data from different bio-geographic regions with various spatial, spectral, and temporal characteristics, and more importantly, the definition of criteria for selecting the most useful method(s) for indicator extraction would benefit the provision of accurate biodiversity indicators in a consistent manner.

Numerous RS methods are assisted by ancillary in-situ information, including field measurements, elevation models, and GIS thematic layers. In many applications, including invasion ecology, phenology, and ecosystem services (He et al. 2011; Ayanu et al. 2012), in-situ data are indispensable for modelling, calibration, training, or validation of the developed RS approaches. Lack of high quality in-situ data, or data collected in inconsistent manner under different sources, periods, or methods, may severely limit the quality of RS products (Gillespie et al. 2008; Xie et al. 2008). Thus, harmonized collection of in-situ data and the

expansion of large scale national or international field data collection initiatives, e.g. the Land Use/Cover Area frame statistical Survey (LUCAS) (Gallego and Bamps 2008), will be crucial steps for RS and in-situ operational integration.

A large spectrum of algorithms is employed for processing and mapping applications, including knowledge and data driven classifiers, and regression analyses. The use of hyperspectral data, backscatter coefficients, and large number of generated spectral or texture features, in both pixel- and object-based approaches, has necessitated the use of feature selection and dimensionality reduction algorithms, with the selection on the most appropriate among those and others depending on the specific application.

As has been recognised, fusion of both active and passive data sources are promising (Nagendra et al. 2013), but also a great challenge for future research (Koch 2010). Wider use of existing and upcoming remote sensing data in operational tasks, integration with high performing algorithms, and broader dissemination of research outcomes will enhance the robustness of biodiversity monitoring and the assessment of the progress towards the achievement of the established preservation targets, at a global scale.

References

2010BIP (2010) Biodiversity indicators and the 2010 Target: Experiences and lessons learnt from the 2010 Biodiversity Indicators Partnership. Tech. Rep. 53, Secretariat of the Convention on Biological Diversity, Montreal

Abbas A, Khan S, Hussain N, Hanjra MA, Akbar S (2013) Characterizing soil salinity in irrigated agriculture using a remote sensing approach. Phys Chem Earth Pt A/B/C 55-57:43–52

Adam E, Mutanga O, Rugege D (2009) Multispectral and hyperspectral remote sensing for identification and mapping of wetland vegetation: a review. Wetl Ecol Manag 18(3):281–296

Adamo M, Tarantino C, Kosmidou V, et al. (2013) Land cover to habitat map translation: Disambiguation rules based on Earth Observation data. In: Int. Geoscience and Remote Sensing Symp., IEEE, Melbourne, pp 3817–3820

Adamo M, Tarantino C, Tomaselli V, et al. (2014) Expert knowledge for translating land cover/use maps to General Habitat Categories (GHC). Landscape Ecol 29(6):1045–1067

AHTEG (2011) Report of the Ad Hoc Technical Expert Group on Indicators for the Strategic Plan for Biodiversity 2011-2020. Tech. rep., Ad Hoc Technical Expert Group on Indicators for the Strategic Plan for Biodiversity 2011-2020, High Wycombe, United Kingdom

Alcantara C, Kuemmerle T, Prishchepov AV, Radeloff VC (2012) Mapping abandoned agriculture with multi-temporal MODIS satellite data. Remote Sens Environ 124:334–347

Altamirano A, Field R, Cayuela L, et al. (2010) Woody species diversity in temperate Andean forests: The need for new conservation strategies. Biol Conserv 143(9):2080–2091

Arias-González JE, Acosta-González G, Membrillo N, Garza-Pérez JR, Castro-Pérez JM (2011) Predicting spatially explicit coral reef fish abundance, richness and Shannon-Weaver index from habitat characteristics. Biodivers Conserv 21(1):115–130

Artigas F, Pechmann IC (2010) Balloon imagery verification of remotely sensed Phragmites australis expansion in an urban estuary of New Jersey, USA. Landscape Urban Plan 95(3):105–112

Atkinson PM, Pardo-Igúzquiza E, Chica-Olmo M (2008) Downscaling cokriging for super-resolution mapping of continua in remotely sensed images. IEEE T Geosci Remote 46(2):573–580

Ayanu YZ, Conrad C, Nauss T, Wegmann M, Koellner T (2012) Quantifying and mapping ecosystem services supplies and demands: a review of remote sensing applications. Environ Sci Technol 46(16):8529–8541

Baldeck CA, Colgan MS, Féret JB, et al. (2014) Landscape-scale variation in plant community composition of an African savanna from airborne species mapping. Ecol Appl 24(1):84–93

Balvanera P, Pfisterer AB, Buchmann N, et al. (2006) Quantifying the evidence for biodiversity effects on ecosystem functioning and services. Ecol Lett 9(10):1146–1156

Banskota A, Wynne RH, Johnson P, Emessiene B (2011) Synergistic use of very high-frequency radar and discrete-return lidar for estimating biomass in temperate hardwood and mixed forests. Ann For Sci 68(2):347–356

Bechle MJ, Millet DB, Marshall JD (2013) Remote sensing of exposure to NO_2: Satellite versus ground-based measurement in a large urban area. Atmos Environ 69(2):345–353

Bejarano S, Mumby PJ, Sotheran I (2010) Predicting structural complexity of reefs and fish abundance using acoustic remote sensing (RoxAnn). Mar Biol 158(3):489–504

Bellard C, Bertelsmeier C, Leadley P, Thuiller W, Courchamp F (2012) Impacts of climate change on the future of biodiversity. Ecol Lett 15:365–377

Belluco E, Camuffo M, Ferrari S, et al. (2006) Mapping salt-marsh vegetation by multispectral and hyperspectral remote sensing. Remote Sens Environ 105(1):54–67

Berberoglu S, Akin A (2009) Assessing different remote sensing techniques to detect land use/cover changes in the eastern Mediterranean. Int J Appl Earth Obs 11(1):46–53

Bergen KM, Gilboy AM, Brown DG (2007) Multi-dimensional vegetation structure in modeling avian habitat. Ecol Inform 2(1):9–22

Bergen KM, Goetz SJ, Dubayah RO, et al. (2009) Remote sensing of vegetation 3-D structure for biodiversity and habitat: Review and implications for lidar and radar spaceborne missions. J Geophys Res 114:G00E06

Blaschke T (2010) Object based image analysis for remote sensing. ISPRS J Photogramm 65(1):2–16

Blaschke T, Lang S, Hay GJ (eds) (2008) Object-Based Image Analysis: Spatial Concepts for Knowledge-Driven Remote Sensing Applications. Springer-Verlag, Berlin Heidelberg

Blonda P, Lucas R, Inglada J, et al. (2013) Copernicus Biodiversity Monitoring Services: The FP7 SPACE projects perspective. White Paper. URL http://www.biosos.eu/publ/White_Paper_Biodiversity_Monitoring_BIOSOS_MSMONINA.pdf

Bock M, Xofis P, Mitchley J, Rossner G, Wissen M (2005) Object-oriented methods for habitat mapping at multiple scales – Case studies from Northern Germany and Wye Downs, UK. J Nat Conserv 13(2–3):75–89

Boyd DS, SanchezHernandez C, Foody GM (2006) Mapping a specific class for priority habitats monitoring from satellite sensor data. Int J Remote Sens 27(13):2631–2644

Brooks TM, Mittermeier RA, da Fonseca GAB, Gerlach J, Hoffmann M (2006) Global biodiversity conservation priorities. Science 313:58–61

Brzank A, Heipke C, Goepfert J (2008a) Morphologic change detection in the Wadden Sea from lidar data. In: International Archives of the Photogrammetry, Remote Sensing and Spatial Information Sciences, ISPRS, Beijing, pp 647–652

Brzank A, Heipke C, Goepfert J, Soergel U (2008b) Aspects of generating precise digital terrain models in the Wadden Sea from lidarwater classification and structure line extraction. ISPRS J Photogramm Remote Sens 63(5):510–528

Buchanan G, Pearce-Higgins J, Grant M, Robertson D, Waterhouse T (2005) Characterization of moorland vegetation and the prediction of bird abundance using remote sensing. J Biogeogr 32(4):697–707

Buchanan GM, Nelson A, Mayaux P, Hartley A, Donald PF (2009) Delivering a global, terrestrial, biodiversity observation system through remote sensing. Conserv Biol 23(2):499–502

Butchart SHM, Walpole M, Collen B, et al. (2010) Global biodiversity: indicators of recent declines. Science 328(5982):1164–1168

Bwangoy JRB, Hansen MC, Roy DP, Grandi GD, Justice CO (2010) Wetland mapping in the Congo Basin using optical and radar remotely sensed data and derived topographical indices. Remote Sens Environ 114(1):73–86

Cardinale BJ, Duffy JE, Gonzalez A, et al. (2012) Biodiversity loss and its impact on humanity. Nature 486:59–67

CBD (2010) Report of the tenth meeting of the conference of the parties to the convention on biological diversity. Tech. rep., Convention on Biological Diversity, Nagoya, Japan

CBD (2012) Report of the eleventh meeting of the conference of the parties to the convention on biological diversity. Tech. rep., Convention on Biological Diversity, Hyderabad, India

Chan JCW, Beckers P, Spanhove T, Vanden Borre J (2012) An evaluation of ensemble classifiers for mapping Natura 2000 heathland in Belgium using spaceborne angular hyperspectral (CHRIS/Proba) imagery. Int J Appl Earth Obs 18:13–22

Chen P, Haboudane D, Tremblay N, et al. (2010) New spectral indicator assessing the efficiency of crop nitrogen treatment in corn and wheat. Remote Sens Environ 114(9):1987–1997

Chen S, Fang L, Zhang L, Huang W (2009) Remote sensing of turbidity in seawater intrusion reaches of Pearl River Estuary A case study in Modaomen water way, China. Estuar Coast Shelf S 82(1):119–127

Chen Z, Muller-Karger FE, Hu C (2007) Remote sensing of water clarity in Tampa Bay. Remote Sens Environ 109(2):249–259

Chi M, Feng R, Bruzzone L (2008) Classification of hyperspectral remote-sensing data with primal SVM for small-sized training dataset problem. Adv Space Res 41(11):1793–1799

Cho MA, Skidmore AK, Sobhan I (2009) Mapping beech (*Fagus sylvatica* L.) forest structure with airborne hyperspectral imagery. Int J Appl Earth Obs 11(3):201–211

Cho MA, Debba P, Mutanga O, et al. (2012) Potential utility of the spectral red-edge region of SumbandilaSat imagery for assessing indigenous forest structure and health. Int J Appl Earth Obs 16:85–93

Clark ML, Roberts DA (2012) Species-level differences in hyperspectral metrics among tropical rainforest trees as determined by a tree-based classifier. Remote Sens 4(12):1820–1855

Clawges R, Vierling K, Vierling L, Rowell E (2008) The use of airborne lidar to assess avian species diversity, density, and occurrence in a pine/aspen forest. Remote Sens Environ 112(5):2064–2073

Colgan M, Baldeck C, Féret JB, Asner G (2012) Mapping savanna tree species at ecosystem scales using support vector machine classification and BRDF correction on airborne hyperspectral and LiDAR data. Remote Sens 4(12):3462–3480

Coops NC, Waring RH, Wulder MA, White JC (2009) Prediction and assessment of bark beetle-induced mortality of lodgepole pine using estimates of stand vigor derived from remotely sensed data. Remote Sens Environ 113(5):1058–1066

Cornforth W, Fatoyinbo T, Freemantle T, Pettorelli N (2013) Advanced Land Observing Satellite Phased Array type L-band SAR (ALOS PALSAR) to inform the conservation of mangroves: Sundarbans as a case study. Remote Sens 5(1):224–237

Costanza R, de Groot R, Sutton P, et al. (2014) Changes in the global value of ecosystem services. Global Environ Change 26:152–158

Debeurs K, Townsend P (2008) Estimating the effect of gypsy moth defoliation using MODIS. Remote Sens Environ 112(10):3983–3990

Delalieux S, Somers B, Haest B, et al. (2012) Heathland conservation status mapping through integration of hyperspectral mixture analysis and decision tree classifiers. Remote Sens Environ 126:222–231

Demir B, Bovolo F, Bruzzone L (2013) Updating land-cover maps by classification of image time series: A novel change-detection-driven transfer learning approach. IEEE T Geosci Remote 51(1):300–312

Dente L, Satalino G, Mattia F, Rinaldi M (2008) Assimilation of leaf area index derived from ASAR and MERIS data into CERES-Wheat model to map wheat yield. Remote Sens Environ 112(4):1395–1407

Dorigo W, Lucieer A, Podobnikar T, Čarni A (2012) Mapping invasive *Fallopia japonica* by combined spectral, spatial, and temporal analysis of digital orthophotos. Int J Appl Earth Obs 19:185–195

Dubinin M, Potapov P, Lushchekina A, Radeloff VC (2010) Reconstructing long time series of burned areas in arid grasslands of southern Russia by satellite remote sensing. Remote Sens Environ 114(8):1638–1648

Duelli P, Obrist MK (2003) Biodiversity indicators: the choice of values and measures. Agr Ecosyst Environ 98(1–3):87–98

Duncanson L, Niemann K, Wulder M (2010) Estimating forest canopy height and terrain relief from GLAS waveform metrics. Remote Sens Environ 114(1):138–154

Duro DC, Coops NC, Wulder MA, Han T (2007) Development of a large area biodiversity monitoring system driven by remote sensing. Prog Phys Geog 31(3):235–260

Duro DC, Girard J, King DJ, et al. (2014) Predicting species diversity in agricultural environments using Landsat TM imagery. Remote Sens Environ 144:214–225

EEA (2007) Halting the loss of biodiversity by 2010: proposal for a first set of indicators to monitor progress in europe. Tech. Rep. 11, European Environment Agency, Copenhagen

EEA (2012a) The impacts of invasive alien species in europe. Tech. Rep. 16, European Environment Agency, Copenhagen

EEA (2012b) Streamlining european biodiversity indicators 2020: Building a future on lessons learnt from the sebi 2010 process. Tech. Rep. 11, European Environment Agency, Copenhagen

Evans TL, Costa M, Telmer K, Silva TSF (2010) Using ALOS/PALSAR and RADARSAT-2 to map land cover and seasonal inundation in the Brazilian Pantanal. IEEE J Sel Top Appl 3(4):560–575

Eysn L, Hollaus M, Schadauer K, Pfeifer N (2012) Forest delineation based on airborne LIDAR data. Remote Sens 4(12):762–783

Fahrig L (2003) Effects of habitat fragmentation on biodiversity. Annu Rev Ecol Evol S 34(1):487–515

Fang H, Liang S, Hoogenboom G (2011) Integration of MODIS LAI and vegetation index products with the CSM-CERES-Maize model for corn yield estimation. Int J Remote Sens 32(4):1039–1065

Feld CK, da Silva PM, Sousa JP, et al. (2009) Indicators of biodiversity and ecosystem services: a synthesis across ecosystems and spatial scales. Oikos 118(12):1862–1871

Féret JB, Asner GP (2013) Tree species discrimination in tropical forests using airborne imaging spectroscopy. IEEE T Geosci Remote 51(1):73–84

Fingas M, Brown C (2014) Review of oil spill remote sensing. Mar Pollut Bull 83(1):9–23

Flanders D, Hall-Beyer M, Pereverzoff J (2003) Preliminary evaluation of eCognition object-based software for cut block delineation and feature extraction. Can J Remote

Sens 29(4):441–452
Forzieri G, Tanteri L, Moser G, Catani F (2013) Mapping natural and urban environments using airborne multi-sensor ADS40-MIVIS-LiDAR synergies. Int J Appl Earth Obs 23:313–323
Franke J, Navratil P, Keuck V, Peterson K, Siegert F (2012) Monitoring fire and selective logging activities in tropical peat swamp forests. IEEE J Sel Top Appl 5(6):1811–1820
Fretwell PT, Trathan PN (2009) Penguins from space: faecal stains reveal the location of emperor penguin colonies. Global Ecol Biogeogr 18(5):543–552
Fretwell PT, Larue MA, Morin P, et al. (2012) An emperor penguin population estimate: the first global, synoptic survey of a species from space. PloS One 7(4):e33,751
Fretwell PT, Staniland IJ, Forcada J (2014) Whales from space: counting southern right whales by satellite. PloS One 9(2):e88,655
Fuchs H, Magdon P, Kleinn C, Flessa H (2009) Estimating aboveground carbon in a catchment of the Siberian forest tundra: Combining satellite imagery and field inventory. Remote Sens Environ 113(3):518–531
Fuentes D, Gamon J, Cheng Y, et al. (2006) Mapping carbon and water vapor fluxes in a chaparral ecosystem using vegetation indices derived from AVIRIS. Remote Sens Environ 103(3):312–323
Gallego J, Bamps C (2008) Using CORINE land cover and the point survey LUCAS for area estimation. Int J Appl Earth Obs 10(4):467–475
García M, Riaño D, Chuvieco E, Danson FM (2010) Estimating biomass carbon stocks for a Mediterranean forest in central Spain using LiDAR height and intensity data. Remote Sens Environ 114(4):816–830
García-Gigorro S, Saura S (2005) Forest fragmentation estimated from remotely sensed data: Is comparison across scales possible? Forest Sci 51(1):51–63
Garcia-Pineda O, Zimmer B, Howard M, et al. (2009) Using SAR images to delineate ocean oil slicks with a texture-classifying neural network algorithm (TCNNA). Can J Remote Sens 35(5):411–421
GEO BON (2011) Adequacy of biodiversity observation systems to support the cbd 2020 targets. Tech. rep., Group on Earth Observations Biodiversity Observation Network, Pretoria, South Africa
Ghiyamat A, Shafri HZM, Amouzad Mahdiraji G, Shariff ARM, Mansor S (2013) Hyperspectral discrimination of tree species with different classifications using single- and multiple-endmember. Int J Appl Earth Obs 23:177–191
Gillespie TW, Foody GM, Rocchini D, Giorgi AP, Saatchi S (2008) Measuring and modelling biodiversity from space. Prog Phys Geog 32(2):203–221
Gong Z, Gong H, Zhao W, Li X, Hu Z (2007) Using RS and GIS to monitoring Beijing wetland resources evolution. In: IEEE Int. Geoscience and Remote Sensing Symposium, IEEE, Barcelona, pp 4596–4599
Goodwin BJ (2003) Is landscape connectivity a dependent or independent variable? Landscape Ecol 18(7):687–699
Goodwin NR, Collett LJ (2014) Development of an automated method for mapping fire history captured in Landsat TM and ETM+ time series across Queensland, Australia. Remote Sens Environ 148:206–221
Gorsevski V, Kasischke E, Dempewolf J, Loboda T, Grossmann F (2012) Analysis of the impacts of armed conflict on the Eastern Afromontane forest region on the South Sudan Uganda border using multitemporal Landsat imagery. Remote Sens Environ 118:10–20
Griffiths P, Kuemmerle T, Kennedy RE, et al. (2012) Using annual time-series of Landsat images to assess the effects of forest restitution in post-socialist Romania. Remote Sens

Environ 118:199–214
Grinand C, Rakotomalala F, Gond V, et al. (2013) Estimating deforestation in tropical humid and dry forests in Madagascar from 2000 to 2010 using multi-date Landsat satellite images and the random forests classifier. Remote Sens Environ 139:68–80
Guyon D, Guillot M, Vitasse Y, et al. (2011) Monitoring elevation variations in leaf phenology of deciduous broadleaf forests from SPOT/VEGETATION time-series. Remote Sens Environ 115(2):615–627
Hansen MC, Loveland TR (2012) A review of large area monitoring of land cover change using Landsat data. Remote Sens Environ 122:66–74
Hantson W, Kooistra L, Slim PA (2012) Mapping invasive woody species in coastal dunes in the Netherlands: a remote sensing approach using LIDAR and high-resolution aerial photographs. Appl Veg Sci 15(4):536–547
He KS, Rocchini D, Neteler M, Nagendra H (2011) Benefits of hyperspectral remote sensing for tracking plant invasions. Divers Distrib 17(3):381–392
Herrmann I, Pimstein A, Karnieli A, et al. (2011) LAI assessment of wheat and potato crops by VENμS and Sentinel-2 bands. Remote Sens Environ 115(8):2141–2151
Hestir EL, Khanna S, Andrew ME, et al. (2008) Identification of invasive vegetation using hyperspectral remote sensing in the California Delta ecosystem. Remote Sens Environ 112(11):4034–4047
Hmimina G, Dufrêne E, Pontailler JY, et al. (2013) Evaluation of the potential of MODIS satellite data to predict vegetation phenology in different biomes: An investigation using ground-based NDVI measurements. Remote Sens Environ 132:145–158
Höfle B, Vetter M (2009) Water surface mapping from airborne laser scanning using signal intensity and elevation data. Earth Surf Proc Land 34(12):1635–1649
Hou Z, Xu Q, Tokola T (2011) Use of ALS, Airborne CIR and ALOS AVNIR-2 data for estimating tropical forest attributes in Lao PDR. ISPRS J Photogramm 66(6):776–786
Huang C, Goward SN, Masek JG, et al. (2010) An automated approach for reconstructing recent forest disturbance history using dense Landsat time series stacks. Remote Sens Environ 114(1):183–198
Hufkens K, Friedl M, Sonnentag O, et al. (2012) Linking near-surface and satellite remote sensing measurements of deciduous broadleaf forest phenology. Remote Sens Environ 117:307–321
Hüttich C, Gessner U, Herold M, et al. (2009) On the suitability of MODIS time series metrics to map vegetation types in dry savanna ecosystems: a case study in the Kalahari of NE Namibia. Remote Sens 1(4):620–643
Hyyppä J, Yu X, Hyyppä H, et al. (2012) Advances in forest inventory using airborne laser scanning. Remote Sens 4(12):1190–1207
Immitzer M, Atzberger C, Koukal T (2012) Tree species classification with random forest using very high spatial resolution 8-band WorldView-2 satellite data. Remote Sens 4(12):2661–2693
Jain M, Mondal P, DeFries RS, Small C, Galford GL (2013) Mapping cropping intensity of smallholder farms: A comparison of methods using multiple sensors. Remote Sens Environ 134:210–223
Jaskierniak D, Lane PN, Robinson A, Lucieer A (2011) Extracting LiDAR indices to characterise multilayered forest structure using mixture distribution functions. Remote Sens Environ 115(2):573–585
Jenkins RB, Frazier PS (2010) High-resolution remote sensing of upland swamp boundaries and vegetation for baseline mapping and monitoring. Wetlands 30(3):531–540

Jiang H, Strittholt JR, Frost PA, Slosser NC (2004) The classification of late seral forests in the Pacific Northwest, USA using Landsat ETM+ imagery. Remote Sens Environ 91(3-4):320–331

Jonsson BG, Jonsell M (1999) Exploring potential biodiversity indicators in boreal forests. Biodivers Conserv 8(10):1417–1433

Joshi C, de Leeuw J, van Duren IC (2004) Remote sensing and GIS applications for mapping and spatial modelling of invasive species. In: International Archives of the Photogrammetry, Remote Sensing and Spatial Information Sciences, ISPRS, Istanbul, vol XXXV-B7, pp 669–677

Kabbara N, Benkhelil J, Awad M, Barale V (2008) Monitoring water quality in the coastal area of Tripoli (Lebanon) using high-resolution satellite data. ISPRS J Photogramm 63(5):488–495

Kachelriess D, Wegmann M, Gollock M, Pettorelli N (2014) The application of remote sensing for marine protected area management. Ecol Indic 36:169–177

Kati V, Devillers P, Dufrêne M, et al. (2004) Testing the value of six taxonomic groups as biodiversity indicators at a local scale. Conserv Biol 18(3):667–675

Kayitakire F, Hamel C, Defourny P (2006) Retrieving forest structure variables based on image texture analysis and IKONOS-2 imagery. Remote Sens Environ 102(3-4):390–401

Kefauver SC, Peñuelas J, Ustin S (2013) Using topographic and remotely sensed variables to assess ozone injury to conifers in the Sierra Nevada (USA) and Catalonia (Spain). Remote Sens Environ 139:138–148

Kindlmann P, Burel F (2008) Connectivity measures: a review. Landscape Ecol 23(8):879–890

Kobler A, Džeroski S, Keramitsoglou I (2006) Habitat mapping using machine learning-extended kernel-based reclassification of an Ikonos satellite image. Ecol Model 191(1):83–95

Koch B (2010) Status and future of laser scanning, synthetic aperture radar and hyperspectral remote sensing data for forest biomass assessment. ISPRS J Photogramm 65(6):581–590

Kokaly RF, Couvillion BR, Holloway JM, et al. (2013) Spectroscopic remote sensing of the distribution and persistence of oil from the Deepwater Horizon spill in Barataria Bay marshes. Remote Sens Environ 129:210–230

Koy K, McShea WJ, Leimgruber P, Haack BN, Aung M (2005) Percentage canopy cover – using Landsat imagery to delineate habitat for Myanmar's endangered Eld's deer (*Cervus eldi*). Anim Conserv 8(3):289–296

Kronseder K, Ballhorn U, Böhm V, Siegert F (2012) Above ground biomass estimation across forest types at different degradation levels in Central Kalimantan using LiDAR data. Int J Appl Earth Obs 18:37–48

Kuemmerle T, Chaskovskyy O, Knorn J, et al. (2009) Forest cover change and illegal logging in the Ukrainian Carpathians in the transition period from 1988 to 2007. Remote Sens Environ 113(6):1194–1207

Kugler F, Schulze D, Hajnsek I, Pretzsch H, Papathanassiou KP (2014) TanDEM-X Pol-InSAR performance for forest height estimation. IEEE T Geosci Remote 52(10):6404–6422

Kumar S, Simonson SE, Stohlgren TJ (2009) Effects of spatial heterogeneity on butterfly species richness in Rocky Mountain National Park, CO, USA. Biodiv Conserv 18(3):739–763

Kumar T, Patnaik C (2013) Discrimination of mangrove forests and characterization of adjoining land cover classes using temporal C-band Synthetic Aperture Radar data: A case study of Sundarbans. Int J Appl Earth Obs 23:119–131

Laba M, Downs R, Smith S, et al. (2008) Mapping invasive wetland plants in the Hudson River National Estuarine Research Reserve using Quickbird satellite imagery. Remote Sens Environ 112(1):286–300

Lang MW, McCarty GW (2009) Lidar intensity for improved detection of inundation below the forest canopy. Wetlands 29(4):1166–1178

Lang MW, Kasischke ES, Prince SD, Pittman KW (2008) Assessment of C-band synthetic aperture radar data for mapping and monitoring Coastal Plain forested wetlands in the Mid-Atlantic Region, U.S.A. Remote Sens Environ 112(11):4120–4130

Langner A, Samejima H, Ong RC, Titin J, Kitayama K (2012) Integration of carbon conservation into sustainable forest management using high resolution satellite imagery: A case study in Sabah, Malaysian Borneo. Int J Appl Earth Obs 18:305–312

Latifi H, Nothdurft A, Koch B (2010) Non-parametric prediction and mapping of standing timber volume and biomass in a temperate forest: application of multiple optical/LiDAR-derived predictors. Forestry 83(4):395–407

Laurance WF, Useche DC, Rendeiro J, et al. (2012) Averting biodiversity collapse in tropical forest protected areas. Nature 489(7415):290–294

Lechner A, Fletcher A, Johansen K, Erskine P (2012) Characterising upland swamps using object-based classification methods and hyper-spatial resolution imagery derived from an unmanned aerial vehicle. In: ISPRS Annals of Photogrammetry, Remote Sensing and Spatial Information Sciences, ISPRS, Melbourne, vol I-4, pp 101–106

Leifer I, Lehr WJ, Simecek-Beatty D, et al. (2012) State of the art satellite and airborne marine oil spill remote sensing: Application to the BP Deepwater Horizon oil spill. Remote Sens Environ 124:185–209

Liesenberg V, Gloaguen R (2013) Evaluating SAR polarization modes at L-band for forest classification purposes in Eastern Amazon, Brazil. Int J Appl Earth Obs 21:122–135

Lindberg E, Hollaus M (2012) Comparison of methods for estimation of stem volume, stem number and basal area from airborne laser scanning data in a hemi-boreal forest. Remote Sens 4(12):1004–1023

Lindenmayer DB, Margules CR, Botkin DB (2000) Indicators of biodiversity for ecologically sustainable forest management. Conserv Biol 14(4):941–950

Liu S, Dong Y, Deng L, et al. (2014) Forest fragmentation and landscape connectivity change associated with road network extension and city expansion: A case study in the Lancang River Valley. Ecol Indic 36:160–168

Longépé N, Rakwatin P, Isoguchi O, Shimada M (2011) Assessment of ALOS PALSAR 50 m orthorectified FBD data for regional land cover classification by Support Vector Machines. IEEE T Geosci Remote 49(6):2135–2150

Lucas R, Blonda P, Bunting P, et al. (2015) The Earth Observation Data for Habitat Monitoring (EODHaM) system. Int J Appl Earth Obs 37:17–28

Lucas RM, Medcalf K, Brown A, et al. (2011) Updating the Phase 1 habitat map of Wales, UK, using satellite sensor data. ISPRS J Photogramm 66(1):81–102

Lück-Vogel M, OFarrell PJ, Roberts W (2013) Remote sensing based ecosystem state assessment in the Sandveld Region, South Africa. Ecol Indic 33:60–70

Lynch J, Maslin M, Balzter H, Sweeting M (2013) Choose satellites to monitor deforestation. Nature 496(7445):293–294

Maes J, Teller A, Erhard M, et al. (2013) Mapping and Assessment of Ecosystems and their Services: An analytical framework for ecosystem assessments under action 5 of the EU biodiversity strategy to 2020. Tech. rep., Publications office of the European Union, Luxembourg

Maghsoudi Y, Collins M, Leckie DG (2012) Polarimetric classification of Boreal forest using nonparametric feature selection and multiple classifiers. Int J Appl Earth Obs 19:139–150

Mairota P, Cafarelli B, Labadessa R, et al. (2015) Very high resolution earth observation features for monitoring plant and animal community structure across multiple spatial scales in protected areas. Int J Appl Earth Obs 37:100–105

Manakos I, Schneider T, Ammer U (2000) A comparison between the ISODATA and the eCognition classification methods on basis of field data. In: International Archives of Photogrammetry and Remote Sensing, ISPRS, Amsterdam, vol XXXIII (Supplement B7), pp 133–139

Martín-Martín C, Bunce RG, Saura S, Elena-Rosselló R (2013) Changes and interactions between forest landscape connectivity and burnt area in Spain. Ecol Indic 33:129–138

Martínez-López J, Carreño M, Palazón-Ferrando J, Martínez-Fernández J, Esteve M (2014) Remote sensing of plant communities as a tool for assessing the condition of semiarid Mediterranean saline wetlands in agricultural catchments. Int J Appl Earth Obs 26:193–204

McDermid GJ, Franklin SE, LeDrew EF (2005) Remote sensing for large-area habitat mapping. Prog Phys Geog 29(4):449–474

McGarigal K, Cushman SA, Ene E (2012) FRAGSTATS v4: Spatial pattern analysis program for categorical and continuous maps. Computer software program. University of Massachusetts, Amherst. Available at http://www.umass.edu/landeco/research/fragstats/fragstats.html

Melin M, Packalén P, Matala J, Mehtätalo L, Pusenius J (2013) Assessing and modeling moose (*Alces alces*) habitats with airborne laser scanning data. Int J Appl Earth Obs 23:389–396

Mera D, Cotos JM, Varela-Pet J, Garcia-Pineda O (2012) Adaptive thresholding algorithm based on SAR images and wind data to segment oil spills along the northwest coast of the Iberian Peninsula. Mar Pollut Bull 64(10):2090–2096

Miao X, Gong P, Swope S, et al. (2006) Estimation of yellow starthistle abundance through CASI-2 hyperspectral imagery using linear spectral mixture models. Remote Sens Environ 101(3):329–341

Moriondo M, Maselli F, Bindi M (2007) A simple model of regional wheat yield based on NDVI data. Eur J Agron 26(3):266–274

Motohka T, Shimada M, Uryu Y, Setiabudi B (2014) Using time series PALSAR gamma nought mosaics for automatic detection of tropical deforestation: A test study in Riau, Indonesia. Remote Sens Environ In press

Muad AM, Foody GM (2012) Super-resolution mapping of lakes from imagery with a coarse spatial and fine temporal resolution. Int J Appl Earth Obs 15:79–91

Müller J, Brandl R (2009) Assessing biodiversity by remote sensing in mountainous terrain: the potential of LiDAR to predict forest beetle assemblages. J Appl Ecol 46(4):897–905

Mwita E, Menz G, Misana S, et al. (2013) Mapping small wetlands of Kenya and Tanzania using remote sensing techniques. Int J Appl Earth Obs 21:173–183

Nagendra H (2001) Using remote sensing to assess biodiversity. Int J Remote Sens 22(12):2377–2400

Nagendra H, Lucas R, Honrado JP, et al. (2013) Remote sensing for conservation monitoring: Assessing protected areas, habitat extent, habitat condition, species diversity, and threats. Ecol Indic 33:45–59

Nelson R, Ranson K, Sun G, et al. (2009) Estimating Siberian timber volume using MODIS and ICESat/GLAS. Remote Sens Environ 113(3):691–701

Newman ME, McLaren KP, Wilson BS (2014) Assessing deforestation and fragmentation in a tropical moist forest over 68 years; the impact of roads and legal protection in the Cockpit Country, Jamaica. Forest Ecol Manag 315:138–152

Nichol JE, Sarker MLR (2011) Improved biomass estimation using the texture parameters of two high-resolution optical sensors. IEEE T Geosci Remote 49(3):930–948

Olmanson LG, Bauer ME, Brezonik PL (2008) A 20-year Landsat water clarity census of Minnesota's 10,000 lakes. Remote Sens Environ 112(11):4086–4097

Ozdemir I, Karnieli A (2011) Predicting forest structural parameters using the image texture derived from WorldView-2 multispectral imagery in a dryland forest, Israel. Int J Appl Earth Obs 13(5):701–710

Pan Z, Yu J, Huang H, et al. (2013) Super-resolution based on compressive sensing and structural self-similarity for remote sensing images. IEEE T Geosci Remote 51(9):4864–4876

Paneque-Gálvez J, Mas JF, Moré G, et al. (2013) Enhanced land use/cover classification of heterogeneous tropical landscapes using support vector machines and textural homogeneity. Int J Appl Earth Obs 23:372–383

Patel RC, Joshi MV (2015) Super-resolution of hyperspectral images: Use of optimum wavelet filter coefficients and sparsity regularization. IEEE T Geosci Remote 53(4):1728–1736

Pengra BW, Johnston Ca, Loveland TR (2007) Mapping an invasive plant, Phragmites australis, in coastal wetlands using the EO-1 Hyperion hyperspectral sensor. Remote Sens Environ 108(1):74–81

Pereira HM, Navarro LM, Martins IS (2012) Global biodiversity change: The bad, the good, and the unknown. Annu Rev Env Resour 37:25–50

Pereira HM, Ferrier S, Walters M, et al. (2013) Essential biodiversity variables. Science 339:277–278

Pérez-Luque AJ, Pérez-Pérez R, Bonet-García FJ, Magaña PJ (2015) An ontological system based on MODIS images to assess ecosystem functioning of Natura 2000 habitats: A case study for Quercus pyrenaica forests. Int J Appl Earth Obs 37:142–151

Perry EM, Fitzgerald GJ, Nuttall JG, et al. (2012) Rapid estimation of canopy nitrogen of cereal crops at paddock scale using a Canopy Chlorophyll Content Index. Field Crop Res 134:158–164

Petrou ZI, Tarantino C, Adamo M, Blonda P, Petrou M (2012) Estimation of vegetation height through satellite image texture analysis. In: International Archives of the Photogrammetry, Remote Sensing and Spatial Information Sciences, Melbourne, vol XXXIX-B8, pp 321–326

Petrou ZI, Kosmidou V, Manakos I, et al. (2014) A rule-based classification methodology to handle uncertainty in habitat mapping employing evidential reasoning and fuzzy logic. Pattern Recogn Lett 48:24–33

Pettorelli N, Laurance WF, O'Brien TG, et al. (2014) Satellite remote sensing for applied ecologists: opportunities and challenges. J Appl Ecol 51:839–848

Pittiglio C, Skidmore AK, van Gils HAMJ, Prins HH (2012) Identifying transit corridors for elephant using a long time-series. Int J Appl Earth Obs 14(1):61–72

Plexida SG, Sfougaris AI, Ispikoudis IP, Papanastasis VP (2014) Selecting landscape metrics as indicators of spatial heterogeneityA comparison among Greek landscapes. Int J Appl Earth Obs 26:26–35

Pontius J, Martin M, Plourde L, Hallett R (2008) Ash decline assessment in emerald ash borer-infested regions: A test of tree-level, hyperspectral technologies. Remote Sens Environ 112(5):2665–2676

Popescu SC, Zhao K, Neuenschwander A, Lin C (2011) Satellite lidar vs. small footprint airborne lidar: Comparing the accuracy of aboveground biomass estimates and forest structure metrics at footprint level. Remote Sens Environ 115(11):2786–2797

Price KP, Guo X, Stiles JM (2002) Optimal Landsat TM band combinations and vegetation indices for discrimination of six grassland types in eastern Kansas. Int J Remote Sens 23(23):5031–5042

Pu R, Bell S, Levy KH, Meyer C (2010) Mapping detailed seagrass habitats using satellite imagery. In: IEEE Int. Geoscience and Remote Sensing Symposium, Honolulu, Hi, pp 1–4

Purkis SJ, Graham NAJ, Riegl BM (2008) Predictability of reef fish diversity and abundance using remote sensing data in Diego Garcia (Chagos Archipelago). Coral Reefs 27(1):167–178

Reiche M, Funk R, Zhang Z, et al. (2012) Application of satellite remote sensing for mapping wind erosion risk and dust emission-deposition in Inner Mongolia grassland, China. Grassland Sci 58(1):8–19

Ren J, Chen Z, Zhou Q, Tang H (2008) Regional yield estimation for winter wheat with MODIS-NDVI data in Shandong, China. Int J Appl Earth Obs 10(4):403–413

Renó VF, Novo EM, Suemitsu C, Rennó CD, Silva TS (2011) Assessment of deforestation in the Lower Amazon floodplain using historical Landsat MSS/TM imagery. Remote Sens Environ 115(12):3446–3456

Ryu Y, Lee G, Jeon S, Song Y, Kimm H (2014) Monitoring multi-layer canopy spring phenology of temperate deciduous and evergreen forests using low-cost spectral sensors. Remote Sens Environ 149:227–238

Sandberg G, Ulander L, Fransson J, Holmgren J, Le Toan T (2011) L- and P-band backscatter intensity for biomass retrieval in hemiboreal forest. Remote Sens Environ 115(11):2874–2886

Sano EE, Rosa R, Brito JLS, Ferreira LG (2010) Land cover mapping of the tropical savanna region in Brazil. Environ Monit Assess 166(1–4):113–124

Saura S, Pascual-Hortal L (2007) A new habitat availability index to integrate connectivity in landscape conservation planning: Comparison with existing indices and application to a case study. Landscape Urban Plan 83(2-3):91–103

Schmidt A, Soergel U (2013) Monitoring and change detection of Wadden Sea areas using Lidar data. In: International Archives of the Photogrammetry, Remote Sensing and Spatial Information Sciences, ISPRS, Antalya, vol XL-7/W2, pp 219–224

Scholes RJ, Walters M, Turak E, et al. (2012) Building a global observing system for biodiversity. Curr Opin Env Sustain 4(1):139–146

Schroeder TA, Wulder MA, Healey SP, Moisen GG (2011) Mapping wildfire and clearcut harvest disturbances in boreal forests with Landsat time series data. Remote Sens Environ 115(6):1421–1433

Schuster C, Ali I, Lohmann P, et al. (2011) Towards detecting swath events in TerraSAR-X time series to establish Natura 2000 grassland habitat swath management as monitoring parameter. Remote Sens 3(12):1308–1322

Secades C, O'Connor B, Brown C, Walpole M (2014) Earth Observation for biodiverity Monitoring: A review of current approaches and future opportunities for tracking progress towards the Aichi Biodiversity Targets. Tech. Rep. 72, Secretariat of the Convention on Biological Diversity, Montreal

Sedano F, Kempeneers P, Miguel JS, Strobl P, Vogt P (2013) Towards a pan-European burnt scar mapping methodology based on single date medium resolution optical remote sensing data. Int J Appl Earth Obs 20:52–59

Shahriar Pervez M, Budde M, Rowland J (2014) Mapping irrigated areas in Afghanistan over the past decade using MODIS NDVI. Remote Sens Environ 149:155–165
Shen Z, Liao Q, Hong Q, Gong Y (2012) An overview of research on agricultural non-point source pollution modelling in China. Sep Purif Technol 84:104–111
Shouse M, Liang L, Fei S (2013) Identification of understory invasive exotic plants with remote sensing in urban forests. Int J Appl Earth Obs 21:525–534
Simonson WD, Allen HD, Coomes DA (2013) Remotely sensed indicators of forest conservation status: Case study from a Natura 2000 site in southern Portugal. Ecol Indic 24:636–647
Somers B, Asner GP (2012) Hyperspectral time series analysis of native and invasive species in Hawaiian rainforests. Remote Sens 4(12):2510–2529
Song H, Huang B, Liu Q, Zhang K (2015) Improving the spatial resolution of Landsat TM/ETM+ through fusion with SPOT5 images via learning-based super-resolution. IEEE T Geosci Remote 53(3):1195–1204
Soudani K, François C, le Maire G, Le Dantec V, Dufrêne E (2006) Comparative analysis of IKONOS, SPOT, and ETM+ data for leaf area index estimation in temperate coniferous and deciduous forest stands. Remote Sens Environ 102(1-2):161–175
Strand H, Höft R, Strittholt J, et al. (2007) Sourcebook on Remote Sensing and Biodiversity Indicators. Tech. Rep. 32, Secretariat of the Convention on Biological Diversity, Montreal
Suarez-Seoane S, Osborne PE, Alonso JC (2002) Large-scale habitat selection by agricultural steppe birds in Spain: identifying species-habitat responses using generalized additive models. J Appl Ecol 39(5):755–771
Tang J, Bu K, Yang J, Zhang S, Chang L (2012) Multitemporal analysis of forest fragmentation in the upstream region of the Nenjiang River Basin, Northeast China. Ecol Indic 23:597–607
Thenkabail PS, Enclona EA, Ashton MS, Van Der Meer B (2004) Accuracy assessments of hyperspectral waveband performance for vegetation analysis applications. Remote Sens Environ 91(3–4):354–376
Tilling AK, O'Leary GJ, Ferwerda JG, et al. (2007) Remote sensing of nitrogen and water stress in wheat. Field Crop Res 104(1-3):77–85
Tonolli S, Dalponte M, Neteler M, et al. (2011) Fusion of airborne LiDAR and satellite multispectral data for the estimation of timber volume in the Southern Alps. Remote Sens Environ 115(10):2486–2498
Topouzelis K, Psyllos A (2012) Oil spill feature selection and classification using decision tree forest on SAR image data. ISPRS J Photogramm 68:135–143
Turner W (2013) Satellites: make data freely accessible. Nature 498(7452):37
Turner W, Spector S, Gardiner N, et al. (2003) Remote sensing for biodiversity science and conservation. Trends Ecol Evol 18(6):306–314
Vaglio Laurin G, Liesenberg V, Chen Q, et al. (2013) Optical and SAR sensor synergies for forest and land cover mapping in a tropical site in West Africa. Int J Appl Earth Obs 21:7–16
Vanden Borre J, Paelinckx D, Mücher CA, et al. (2011) Integrating remote sensing in Natura 2000 habitat monitoring: Prospects on the way forward. J Nat Conserv 19(2):116–125
Vastaranta M, Holopainen M, Karjalainen M, et al. (2014) TerraSAR-X stereo radargrammetry and airborne scanning LiDAR height metrics in imputation of forest aboveground biomass and stem volume. IEEE T Geosci Remote 52(2):1197–1204
Vierling KT, Bässler C, Brandl R, et al. (2011) Spinning a laser web: predicting spider distributions using LiDAR. Ecol Appl 21(2):577–588

Virtanen T, Ek M (2014) The fragmented nature of tundra landscape. Int J Appl Earth Obs 27:4–12

Vogeler JC, Hudak AT, Vierling LA, et al. (2014) Terrain and vegetation structural influences on local avian species richness in two mixed-conifer forests. Remote Sens Environ 147:13–22

Vyas D, Krishnayya NSR, Manjunath KR, Ray SS, Panigrahy S (2011) Evaluation of classifiers for processing Hyperion (EO-1) data of tropical vegetation. Int J Appl Earth Obs 13(2):228–235

Walker WS, Stickler CM, Kellndorfer JM, Kirsch KM, Nepstad DC (2010) Large-area classification and mapping of forest and land cover in the Brazilian Amazon: A comparative analysis of ALOS/PALSAR and Landsat data sources. IEEE J Sel Top Appl 3(4):594–604

Walsh SJ, McCleary AL, Mena CF, et al. (2008) QuickBird and Hyperion data analysis of an invasive plant species in the Galapagos Islands of Ecuador: Implications for control and land use management. Remote Sens Environ 112(5):1927–1941

Wang X, Wang Q, Wu C, et al. (2012) A method coupled with remote sensing data to evaluate non-point source pollution in the Xin'anjiang catchment of China. Sci Total Environ 430:132–143

Wang X, Huang H, Gong P, et al. (2014) Forest canopy height extraction in rugged areas with ICESat/GLAS data. IEEE T Geosci Remote 52(8):4650–4657

Wang Z, Huang N, Luo L, et al. (2011) Shrinkage and fragmentation of marshes in the West Songnen Plain, China, from 1954 to 2008 and its possible causes. Int J Appl Earth Obs 13(3):477–486

White JC, Gómez C, Wulder MA, Coops NC (2010) Characterizing temperate forest structural and spectral diversity with Hyperion EO-1 data. Remote Sens Environ 114(7):1576–1589

White K, Pontius J, Schaberg P (2014) Remote sensing of spring phenology in northeastern forests: A comparison of methods, field metrics and sources of uncertainty. Remote Sens Environ 148:97–107

Whittle M, Quegan S, Uryu Y, Stüewe M, Yulianto K (2012) Detection of tropical deforestation using ALOS-PALSAR: A Sumatran case study. Remote Sens Environ 124:83–98

Wijedasa LS, Sloan S, Michelakis DG, Clements GR (2012) Overcoming limitations with Landsat imagery for mapping of peat swamp forests in Sundaland. Remote Sens 4(12):2595–2618

Wolter PT, Townsend PA, Sturtevant BR (2009) Estimation of forest structural parameters using 5 and 10meter SPOT-5 satellite data. Remote Sens Environ 113(9):2019–2036

Wu C, Gonsamo A, Gough CM, Chen JM, Xu S (2014) Modeling growing season phenology in North American forests using seasonal mean vegetation indices from MODIS. Remote Sens Environ 147:79–88

Wulder MA, White JC, Coops NC, Butson CR (2008) Multi-temporal analysis of high spatial resolution imagery for disturbance monitoring. Remote Sens Environ 112(6):2729–2740

Wulder MA, White JC, Nelson RF, et al. (2012) Lidar sampling for large-area forest characterization: A review. Remote Sens Environ 121:196–209

Xie Y, Sha Z, Yu M (2008) Remote sensing imagery in vegetation mapping: a review. J Plant Ecol 1(1):9–23

Yan H, Fu Y, Xiao X, et al. (2009) Modeling gross primary productivity for winter wheat-maize double cropping system using MODIS time series and CO2 eddy flux tower data. Agr Ecosyst Environ 129(4):391–400

Yen KW, Lu HJ, Chang Y, Lee MA (2012) Using remote-sensing data to detect habitat suitability for yellowfin tuna in the Western and Central Pacific Ocean. Int J Remote Sens 33(23):7507–7522

Zainuddin M, Kiyofuji H, Saitoh K, Saitoh SI (2006) Using multi-sensor satellite remote sensing and catch data to detect ocean hot spots for albacore (*Thunnus alalunga*) in the northwestern North Pacific. Deep-Sea Res Pt II 53(3-4):419–431

Zhao D, Cai Y, Jiang H, et al. (2011) Estimation of water clarity in Taihu Lake and surrounding rivers using Landsat imagery. Adv Water Resour 34(2):165–173

Zhao K, Popescu S (2009) Lidar-based mapping of leaf area index and its use for validating GLOBCARBON satellite LAI product in a temperate forest of the southern USA. Remote Sens Environ 113(8):1628–1645

Zhong L, Gong P, Biging GS (2014) Efficient corn and soybean mapping with temporal extendability: A multi-year experiment using Landsat imagery. Remote Sens Environ 140:1–13

Zhu Z, Woodcock CE, Olofsson P (2012) Continuous monitoring of forest disturbance using all available Landsat imagery. Remote Sens Environ 122:75–91

Zlinszky A, Mücke W, Lehner H, Briese C, Pfeifer N (2012) Categorizing wetland vegetation by airborne laser scanning on Lake Balaton and Kis-Balaton, Hungary. Remote Sens 4(12):1617–1650

Zohmann M, Pennerstorfer J, Nopp-Mayr U (2013) Modelling habitat suitability for alpine rock ptarmigan (*Lagopus muta helvetica*) combining object-based classification of IKONOS imagery and Habitat Suitability Index modelling. Ecol Model 254:22–32